

## CHAPTER 12

# *Application of SOFCs in Combined Heat, Cooling and Power Systems*

R. J. BRAUN\* AND P. KAZEMPOOR

Colorado School of Mines, Department of Mechanical Engineering, College of Engineering and Computational Sciences, 1610 Illinois Street, 80401, Golden, Colorado, USA

\*Email: rbraun@mines.edu

## **12.1 Introduction**

The unique characteristics of solid oxide fuel cells (SOFCs) have encouraged their development for a wide variety of applications that range from portable, mobile and micro-combined heat and power (500 W to 20 kW) to larger-scale stationary power at both distributed generation ( $\sim 100$  kW – 5 MW) and central utility scales ( $>100$  MW). Attractive SOFC technology attributes include high electric efficiency, high-grade waste heat, fuel flexibility, low emissions, power scalability, and low unit capital cost potential when high production volumes are achieved. The high operating temperature of SOFCs enable production of varying grades of waste heat that can then be recovered for process heating, power augmentation via gas turbine integration, or for polygeneration of exportable products (*e.g.*, heat, cooling, power or fuels). The effective use of waste heat significantly impacts overall system efficiency, economics and environmental emissions. These attributes have accelerated SOFC technology development with the aim of replacing traditional combustion-based power

---

RSC Energy and Environment Series No. 7

Solid Oxide Fuel Cells: From Materials to System Modeling

Edited by Meng Ni and Tim S. Zhao

© The Royal Society of Chemistry 2013

Published by the Royal Society of Chemistry, [www.rsc.org](http://www.rsc.org)

generation equipment, as well as offering solutions to emerging 21<sup>st</sup> Century energy problems.

While many research studies have been performed on larger-scale (>1 MW) SOFC power systems,<sup>1-4</sup> most of the industrial SOFC hardware technology development activity remains at system capacities of about 250 kW or less. In particular, the current state-of-the-art in SOFC stack power output is in the neighbourhood of 25 kW.<sup>5-7</sup> This technology status has contributed to the near-term focus of SOFC system development for both mobile unmanned aerial and undersea vehicle applications, auxiliary power units (APUs), and combined heat and power (CHP) systems in residential (1–5 kW) and commercial (10–250 kW) building markets. Thus, much of the commercialization activity among SOFC developers is aimed at relatively small-scale applications for mobile systems and residential and light-commercial building CHP (*i.e.*, micro-CHP); the latter of which is predominately occurring in Japan and Europe.<sup>8,9</sup>

### 12.1.1 Drivers for Interest in Co- and Tri-generation Using Fuel Cells

The development of SOFCs as a high-efficiency, low-emission stationary power generator is motivated by the recognition of the technology as a potential cross-cutting solution for a number of emerging paradigms related to energy supply and management. First, dispatchable distributed generation (DG) technologies are one component of a broader set of distributed energy resources (DERs) that are expected to be instrumental in enabling large-scale penetration of intermittent renewable resources, such as wind and solar.<sup>10-13</sup> Key DER technologies envisioned to be significant players in the advancement of distributed generation include fuel cells, micro-turbines, energy storage devices and thermally activated heat recovery technologies (TAT). Large-scale energy storage development is envisioned as a key requirement in being able to both increase the flexibility of and modernize the electric grid, especially in the U.S. In particular, SOFC-derived technologies such as reversible SOFCs and solid oxide electrolysis, are receiving increased interest as candidates to offering viable grid energy storage solutions.<sup>14-16</sup>

Secondly, interest in microgrids as an energy supply and distribution solution to growing reliability and power quality problems associated with the centralized electric grid is also increasing. One of the potential advantages of microgrids is that as a semiautonomous power supply system, it can be controlled and operated as a single aggregated load, while also offering end-users the benefits of meeting their onsite needs for heat, uninterrupted power, and enhanced local reliability and power quality (*e.g.*, via maintaining voltage stability and minimizing harmonic distortion).<sup>11,17</sup> Importantly, the parallel interest and development of microgrid technology is relevant to smaller-scale DG as it can more effectively enable the utilization of waste heat by moving the production of thermal energy closer to the point of end-use.<sup>11</sup> The smaller scale of thermal energy production units also offers flexibility in matching the application requirements for heat and power. Figure 12.1 illustrates the range of DER technologies and their associated

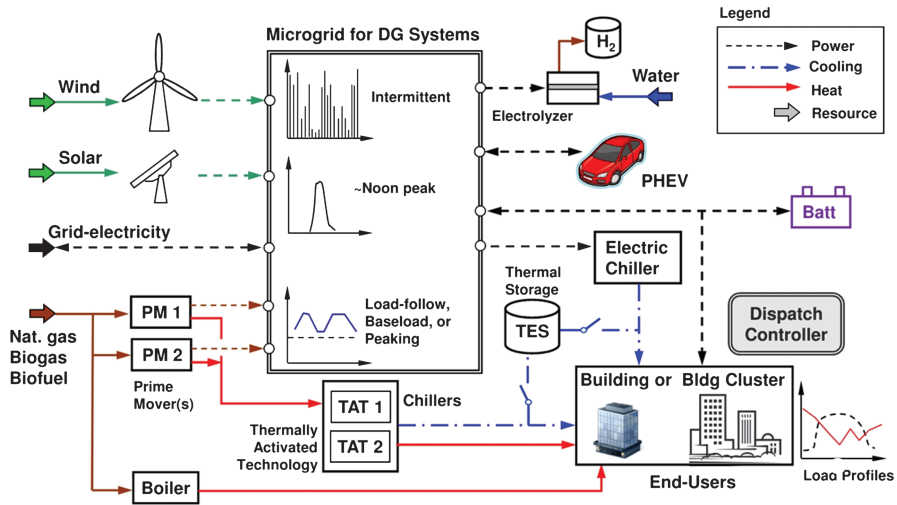


**Figure 12.1** Microgrid with heterogeneous distributed energy resource technologies.

diurnal energy production characteristics that may be employed to serve building or building cluster energy demands. Renewable energy technologies, such as wind and solar, have intermittent production profiles and achieve rather low annual average energy capacity factors (~0.2 to 0.35). Advanced prime movers, such as fuel cells, can be integrated with TAT to provide either cooling (and/or space heating directly) to the end-user or employ thermal energy storage (TES) for later use depending on energy pricing, demand, and overall emissions considerations. Advanced DER technologies, which include fuel (hydrogen) generation via electrolyzers and plug-in hybrid vehicles (PHEV) are also shown. In such energy paradigms of the future, the ability to co- or tri-generate (or ‘polygenerate’) energy products becomes increasingly attractive given the relatively high costs of early production fuel cell DG technologies as it allows the allocation of capital costs to be distributed among all of the various co-products, thereby reducing the unit production costs of each commodity stream. Polygeneration encompasses CHP, combined cooling, heat, and power (CCHP), combined heat, hydrogen, and power (CHHP), and combined fuel and power (CFP). It continues to experience global interest as a means for energy supply security, efficiency enhancement, environmental impact reduction,<sup>†</sup> and as a response to the growing uncertainty in electricity markets due to competition and an overburdened grid infrastructure.<sup>18</sup>

### 12.1.2 Overview of CHP and CCHP

Combined cooling, heat and power is a method whereby a prime mover (such as a fuel cell or stationary engine) consumes fuel to produce power and the

<sup>†</sup>For example, through emission control and avoidance of construction of both large generating plants and the associated transmission and distribution infrastructure.

waste heat rejected from the system is recovered to provide space heating and/or hot water, and cooling which is typically (but not always) derived from a thermally activated technology such as an absorption chiller. In some cases, the term CCHP is employed for situations in which combined cooling, heat and power are not produced simultaneously; but instead heat and power are produced during the heating season, and cooling and power are produced during the cooling season. The primary difference between CHP and CCHP is that excess thermal or mechanical/electrical energy derived from the prime mover is employed to produce cooling for a CCHP application.<sup>19</sup> CCHP is synonymous with tri-generation or building cooling, heating and power (BCHP) and one of its main benefits is the reduction of primary energy necessary to deliver a required amount of electric power and thermal energy over separate production methods.<sup>19,20</sup>

Figure 12.2 depicts a generic SOFC-CHP system where a hydrocarbon fuel, such as natural gas is supplied to the system and electric power and thermal energy are exported to meet end-use requirements of a given application. Figure 12.3 depicts a schematic diagram of a typical CCHP configuration for a fuel cell. Fuel, such as natural gas, is supplied to a fuel cell sub-system and AC electric power is generated. Waste heat from the system is recovered to drive a thermally activated cooling technology (*e.g.*, absorption chiller, adsorption chiller, or desiccant dehumidifier); any remaining un-utilized thermal energy is made available for hot water production. The fuel cell-based CCHP system is comprised of the fuel cell sub-system, power conditioning, heat recovery system and thermally activated cooling hardware. In such a configuration, overall system efficiencies can range from 70–95% to produce three useful energy products compared with the 30–40% from typical coal-fired central utility power plants making electricity alone. In general, a distributed generation CCHP system can readily achieve an overall efficiency of 88–90%, while separate production methods for cooling, heat and power supplies achieve a combined efficiency of less than 60%.<sup>19,21,22</sup> The three commercially available thermally activated cooling technologies are absorption chillers, adsorption chillers and desiccant dehumidifiers. Direct-drive vapour-compression chilling is also available whereby steam-generated from a waste heat recovery boiler is expanded to provide the mechanical shaft power requirements of the

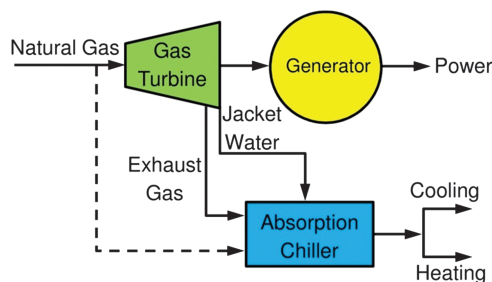


**Figure 12.2** Conventional CCHP system.

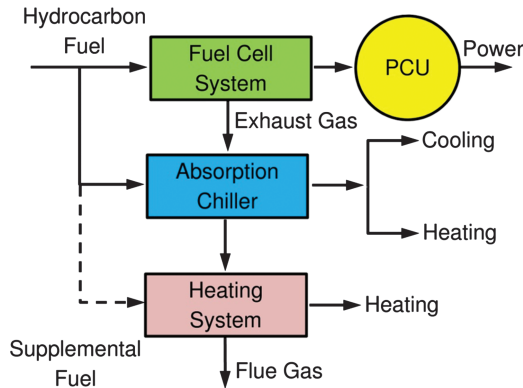


**Figure 12.3** SOFC-CCHP system.

compressor in the refrigeration system. From Figure 12.3, it is apparent that an SOFC-CHP system is nearly identical to a CCHP system, except it does not contain the thermally activated components needed to supply cooling for building air-conditioning loads.

This chapter focuses on the application of SOFC technology in both CHP and CCHP systems for residential and commercial buildings. In particular, modelling approaches, integration strategies, and benefits and challenges for SOFC-based CHP and CCHP systems are presented. The chapter is organized such that a brief overview of building application requirements and economic considerations are first presented. SOFC-based CCHP system configurations and operation are then discussed. Considering the lack of SOFC-CCHP systems either commercially available or in demonstration, the presentation herein has a predominate focus on SOFC-CHP systems at relatively small scales (< 10 kW). Basic modelling approaches and techniques for system design and simulation are given next, followed by a synthesis of results and observations concerning the expected effectiveness of SOFC-CHP systems in the building energy markets. The chapter concludes with an overview of SOFC commercialization efforts, technology and economic barriers, and market outlook.

## 12.2 Application Characteristics & Building Integration

Building types for potential application of SOFC-CHP/CCHP systems are wide ranging and include hotels, hospitals, office buildings, educational institutions, mercantile (*e.g.*, retail), apartments, supermarkets, and single-family residential dwellings to name a few. There are many technical, economic and regulatory factors to consider when determining the suitability of a fuel cell-CHP system for application in residential and commercial buildings including:

- Building electric and thermal load characteristics
- Grid-electricity and natural gas prices and rate structures

- Utility net-metering plans
- Grid-connection requirements and regulations
- Plant siting and permitting

This section only focuses on the technical aspects of SOFC-CHP/CCHP building installations. Building load profiles and building-integrated fuel cell systems are briefly discussed in the following to introduce various application characteristics and to provide some context for subsequent discussions on system configurations, modelling, and market considerations. Economic considerations and market requirements are discussed further in Sections 12.4 and 12.7.

A useful performance characteristic for matching energy supply with energy demand is the thermal-to-electric ratio (TER). The TER of a building structure is the ratio of the thermal energy demand to the base electrical demand. A TER may be based on space heating, space cooling, or domestic hot water demands within a building and its magnitude is highly dependent on location, building type and design, usage patterns, time of day, and time of year.<sup>23</sup> A TER may also be expressed for an SOFC-CHP/CCHP system, in which case the ratio represents the amount of thermal energy available for export divided by the net power generated by the system. The TER of an SOFC-CHP/CCHP system depends on many factors, but in general can range from 0.5 for high electric efficiency systems to almost 2.0 for lower efficiency ones.

### 12.2.1 Commercial Buildings

The electrical and thermal energy demands in commercial buildings vary widely over the course of a day, season, and geographic location. Figure 12.4(a,b) illustrates an example of the diurnal electrical and thermal energy usage of a prototypical large hotel located in southern California on an hourly time-average basis. The energy demand profiles for the buildings and locations depicted in Figure 12.4 were generated using EnergyPlus software<sup>24</sup> and input files for standard building types defined by the U.S. Department of Energy.<sup>25</sup> Figure 12.4(a) shows that electric demand over the course of a winter or summer day can vary by over 220 kW where the minimum load is near 90–110 kW in the early morning hours and as high as 340 kW in the evening hours. The effect of the vapour-compression cooling load is also observable when comparing January and July days, adding as much as 100 kW to the electrical demand in the afternoon hours (which often represent a high price of electricity time period). Over the course of the day, the hourly-average space cooling TER for the building ranges from 0.35 to 1.1 in the winter and from about 1.0 to 2.1 in the summer. Building size and demand characteristics are further summarized in Table 12.1.

The thermal load profiles for the large hotel on a January day are depicted in Figure 12.4(b). In the warm climate of southern California, the building experiences significant cooling and heating loads throughout the day, where the thermal energy demand is primarily in the form of domestic hot water (DHW)

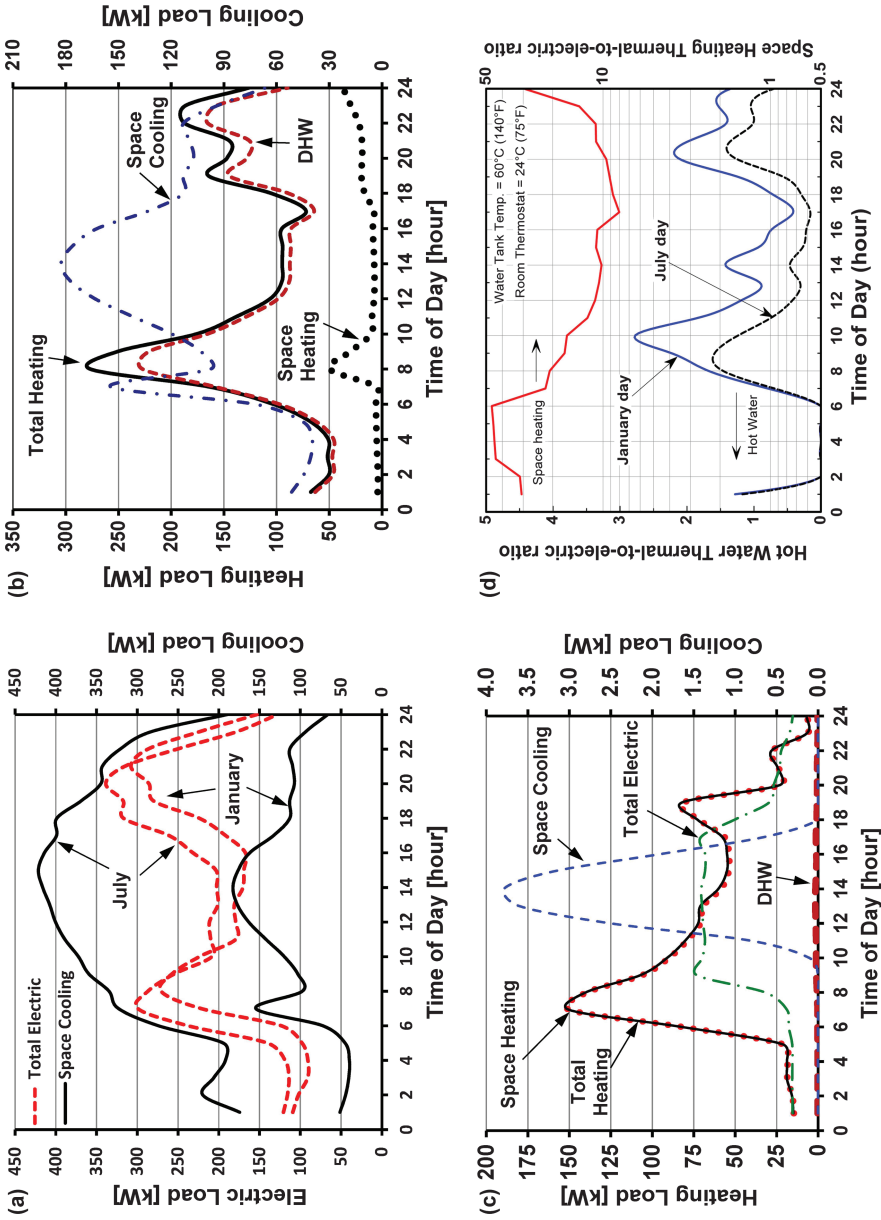


**Figure 12.4** (a) Electric and cooling load profiles of prototypical large hotel in Los Angeles, CA during July and January days; (b) Thermal load profiles for prototypical large hotel in Los Angeles, CA during a January day; (c) Electric and thermal load profiles for prototypical medium office building in Boston, MA; (d) Domestic hot water and space heating TERs for a 230 m<sup>2</sup> residential dwelling located in Madison, WI.

**Table 12.1** Summary of commercial building energy characteristics for a large hotel and medium-office in the U.S.

<i>Statistic</i>	<i>Los Angeles Hotel</i>	<i>Boston Hotel</i>	<i>Los Angeles Office</i>	<i>Boston Office</i>
Height (floors)	6	6	3	3
Area (thousand ft <sup>2</sup> )	122	122	54	54
Average power demand (kW)	204	142	54	53
Maximum power demand (kW)	357	263	151	167
Minimum power demand (kW)	87	52	15	15
Average heating demand (kW)	101	294	12	51
Maximum heating demand (kW)	353	625	81	317
Minimum heating demand (kW)	29	78	0.3	0.3
Average thermal-to-electric ratio (kW)	0.49	2.16	0.29	0.96
Maximum thermal-to-electric ratio (kW)	1.24	4.23	3.1	13.6
Minimum thermal-to-electric ratio (kW)	0.16	0.95	0.01	0.02
Average cooling demand (kW)	204	137	38	29
Maximum cooling demand (kW)	599	796	228	249
Minimum cooling demand (kW)	21	0	0	0

usage. DHW-based TER values range from as low as 0.16 to over 1.2 over the course of the year (see Table 12.1).

The effect of building type and geographic location can be seen from examination of the electric and thermal loads for a medium-sized office building located in Boston, Massachusetts as presented in Figure 12.4c. The winter day loads depicted illustrate a nearly steady daytime electric load of about 65–70 kW and space heating loads exceeding 150 kW during the early morning hours. DHW heating loads are less than 5 kW and a small amount of space cooling (1–3 kW) is still required during a winter day often for cooling of the building interior. Office building TERs can range substantially over the course of a year from effectively zero to over 13 for space heating during the winter.

## 12.2.2 Residential Applications

Similar to commercial buildings, single-family residential applications experience significant variation in both the timing and magnitude of their energy demands. The annual hourly average domestic hot water TER for a ~230 m<sup>2</sup> home in the U.S. can range from 0.7–1.0.<sup>26</sup> Figure 12.4(d) shows the building loads for a prototypical residence located in Madison, Wisconsin during a winter and summer day in terms of TER. Load data was generated using TRNSYS<sup>27</sup> with typical meteorological year weather data. A peak hourly domestic hot water heating TER of less than 2.75 and a base value near 0.4 is apparent in the figure for a typical January day. The peak domestic hot water TER for a July day is about 1.6 with a base value near 0.2. Also, note both the magnitude and rate of change in domestic hot water TER during the early

hours of the day. The annual hourly average domestic hot water TER is about 1.0 and this value is typical of most households in the U.S. In contrast to domestic hot water heating, the TER data for space heating is substantially higher with a peak hourly TER demand near 50 and a base load of seven. The cooling TER registers a maximum of about five during late afternoon hours. Over the course of an entire year, the annual average hourly electric load for the house is approximately 1.0 kW<sub>e</sub>, and the average domestic hot water load is also about 1.0 kW<sub>th</sub>. Residential-scale fuel cell systems typically generate TERs in the range of 0.5–2 and with the use of thermal storage, can be matched to serve domestic hot water heating loads. For micro SOFC-CHP systems, TER production in the range 0.7 to 1.0 is thus preferred for integration as it matches well with the hourly average demand of residential domestic hot water systems in the U.S.

Given the relatively slow transient response capability of SOFCs<sup>28</sup> and end-use load diversity, both thermal and electrical energy storage concepts may be required. In the case of grid-connected, single-family residential dwellings, electrical energy storage can be avoided by using the grid for peak power and fast dynamic power response. Operating strategy and grid-connection issues are interrelated and are discussed later in this chapter.

### 12.2.3 Building Integration & Operating Strategies

#### 12.2.3.1 Building Integration

Integration of SOFC-CHP/CCHP systems within the building envelope requires interconnection with the building HVAC systems. Design and optimization of integrated systems with variable loads and environmental conditions is a complex endeavour and multi-objective in nature. The simple system diagram shown in Figure 12.5 is provided to motivate subsequent

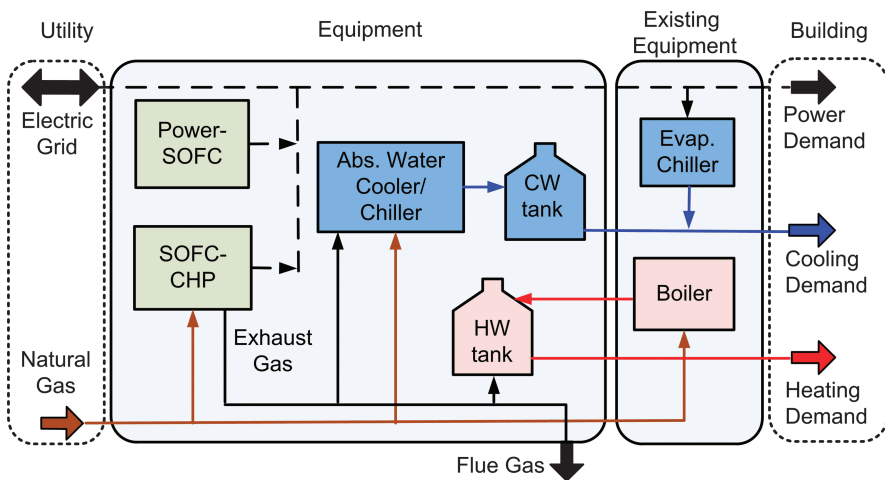


Figure 12.5 Schematic of building-integrated SOFC-CHP/CCHP System.

modelling, design, and optimization discussions. Existing equipment in commercial buildings typically involves electric-driven vapour-compression chilling and natural gas-fired heating systems. Given that most DG systems will not completely serve all thermal and electrical loads of a building, installation of SOFC-based hardware must interface with these systems, irrespective of whether the building is a new construction or a retrofit. As the previous discussion on building load profiles and SOFC TER characteristics demonstrated, some amount of thermal storage and heating capacity is preferred to be able to better match energy demands that are widely disparate. The waste heat from an SOFC power system can be recovered to provide building cooling via absorption chillers and/or to supply hot water for DHW or space heating loads as shown in Figure 12.5. The disparate timing and magnitude of building load profiles mean that thermal storage can be quite important for achieving high overall system efficiency and attractive economics. Thus, both hot and chilled water production can be stored in tanks for later use. Storage can also assist in lowering the capacity requirements of the vapour-compression systems and enable them to be 'right' sized so that they do not operate at the more inefficient part-load conditions for long durations. Hot water production from SOFC-CHP systems can also be used as boiler feedwater preheat, thereby lowering energy production costs. In addition to SOFC-CHP/CCHP systems, Figure 12.5 illustrates that combinations of power-only and CHP SOFC systems could certainly be envisioned if the application requirements are better served by lower TERs, for example.

Application of SOFC-CHP systems in smaller scale buildings, such as residential dwellings, benefit from simpler integration issues. Figure 12.6 illustrates a high-level diagram of how a micro-CHP system might interface with the equipment and loads of a single-family residence and is consistent with the few systems developed practically and/or suggested theoretically.<sup>29-33</sup> The residential energy system shown involves an SOFC system integrated with an auxiliary boiler and storage tank, as well as the heating and cooling systems. The SOFC is the heart of this CCHP system and must produce enough heat and power to economically meet the operating strategy envisioned.<sup>34,35</sup> Although it is theoretically possible to design the SOFC system based on either the maximum heat or power demands, the system cost directly depends on the rated capacity of the SOFC system. In practice, an auxiliary heat generator (*e.g.*, boiler) is required to generate additional heat in the high heat demand periods. Additional electrical demand can also be compensated easily by the grid.<sup>36</sup> Further, in some countries, the SOFC-CHP system could interface with district heating networks.

### 12.2.3.2 Operating Strategies

Selection of an operating/dispatch strategy for application of the fuel cell-CCHP system in a commercial building is important as it strongly affects the economic benefits, efficiency and overall system reliability. Furthermore, it is

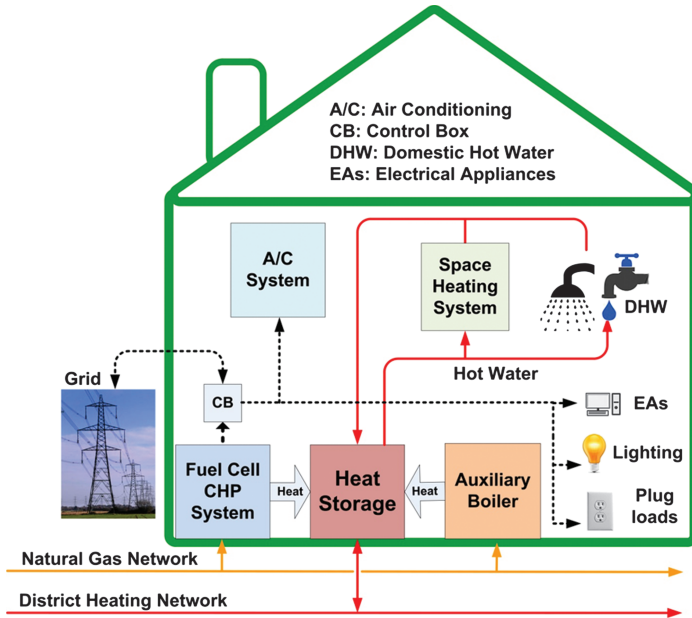


**Figure 12.6** Integration of a fuel cell-CHP system into a residential building.

pre-requisite for proper sizing (*i.e.*, rated capacity) of the CCHP system and for quantifying the value proposition in any given application. The possible operating strategies include (1) electric base-loading of the SOFC system, (2) electric load-following, (3) thermal load-following, (4) seasonal load-following, or (5) peak-shaving.

In an electric base-load strategy, the SOFC-CHP system is operated in a steady-state manner at some nominal power output condition for most of the year. SOFC sizing and base-load operation can be made such that either the system power output does not exceed the expected minimum electric load of building all year or the power output exceeds the minimum building demand for a portion of the day (or year). If surplus power is generated by the SOFC system, it must be exported to the electric grid. If the SOFC-CHP system is base-loaded, then limitations on dynamic performance may be of little concern. When base-loading at rated capacity, the SOFCs are rarely turned down to part load or standby, and do not change power or exhaust gas output between time periods.

In load-following operating strategies, the SOFC system is designed to preferentially meet either the thermal or electrical demands (not both). Thus, the thermal or electrical capacity of the SOFC system exceeds either the minimum electrical or thermal requirement for the facility. With electrical load-following, the fuel cell output power changes in response to the power demand of the building. The thermal demand can be partly supported by the

SOFC system. However, an additional heat source is needed to generate more thermal energy during the high heating demand periods. With a thermal load tracking strategy, the fuel cell system is designed based on the overall heat demand and minimum amount of power required by the facility. During high electrical demand, additional power can be supplied by purchase from the grid.

Seasonal load-following involves a combination of electric and thermal load-following. Under this operating strategy, the CCHP system will operate in either load-following mode for a given month (or season) depending on the monthly (or seasonal) thermal-to-electric ratio of the building.<sup>37</sup> Lastly, a peak shaving CCHP system would call for fuel cell operation only during limited time periods where the time-of-day price of electricity and/or utility demand charges are so high it justifies the limited operation of the DG system.

### 12.3 Overview of SOFC-CHP/CCHP Systems

Much attention is often devoted to the fuel cell only, however, the SOFC is only one component of a relatively complex system. The balance-of-plant (BOP) in an SOFC system typically includes fuel pumps, air blowers, hydrocarbon fuel reformers, tail-gas combustors, and process gas heat exchangers. In fact, the chemistry and transport within components such as the reformer can be as complex as those within the SOFC.<sup>38</sup> Key system parameters such as performance at full and part loads (electrical, thermal and CCHP efficiencies), durability, reliability and capital cost depend strongly on the BOP and its integration with the SOFC stack. For example, it has been shown that the overall system electrical efficiency for a CCHP system is almost 20–35% lower than the stack efficiency.<sup>23,39</sup> The majority of these losses belong to auxiliary power consumption and inefficiency in fuel processing. Losses in the thermal components as well as the power conditioning units are also very important.<sup>26,40</sup> Consequently, the implementation of more efficient components and their optimal integration within the system have an appreciable effect on overall cost and benefits. This optimization is often accomplished by techno-economic modelling and design, which evaluates the most appropriate system configuration and establishes the corresponding optimal operating conditions through minimization of life cycle costs.<sup>41</sup>

In the following sub-section, brief overviews of system components, configurations, and operation are given. The central focus is on the SOFC system as the primary thermal energy and power generator, and thus, details regarding the building cooling and heating systems are not presented here. Importantly, the system presentation provides context for the subsequent discussion of modelling and application techniques for SOFC-CHP/CCHP systems in building applications. Additionally, the following overview proves to be useful in apprehending and evaluating the various operational and

commercial SOFC-CHP systems in development as summarized in Section 12.6 of this chapter.

### 12.3.1 SOFC System Description for CHP (Co-generation)

A process flowsheet for a natural gas fuelled SOFC is shown in Figure 12.7.<sup>23,39</sup> In this system, pressurized fuel is shown to enter a desulfurizer in order to remove the sulfur compounds normally contained in utility provided natural gas at state point (2). The cleaned natural gas (3) is then mixed with superheated steam provided by anode exhaust gas recycling (6) via an ejector to achieve the necessary steam-to-carbon ratio for fuel reforming without carbon deposition. A portion of the fuel pre-heating is also accomplished by the direct mixing of anode tail-gas with the entering fresh fuel. The fuel gas mixture (4) is then passed through an external pre-reformer, which further preheats the mixture and converts a fraction of the natural gas to hydrogen and carbon monoxide before entering the anode compartment of the cell-stack at (5). The thermal energy required to support the endothermic reforming reactions is supplied by the hot exhaust gases leaving the catalytic tail-gas combustor (15). SOFCs are air-cooled and thus, air at near-ambient conditions enters the system in excess of stoichiometric requirements via the blower (8). A portion of the pressurized air flow may be bypassed to control the burner exhaust or inlet cathode temperatures. However, the majority of the airflow is preheated by the burner exhaust gas (11). As an option, an ejector or high-temperature recycle blower may be used to recirculate a fraction of the cathode gas (13) for air pre-heating, while also reducing the size of the air preheat heat exchanger. After electrochemical oxidation of the fuel within the anode, the residual combustibles in the anode tail-gas are mixed with excess air from the cathode exhaust and catalytically oxidized in the tail-gas burner. The burner exhaust gas (15) is the highest temperature (850–1000 °C) in the system and serves as the thermal energy source stream for the downstream process gas reactors and heat exchangers. The dashed lines in Figure 12.7 indicate process flow diagrams for system concepts that may employ anode and/or cathode gas recycle.

The DC power produced by the SOFC stack must be converted into AC power (single- or three-phase, 50 or 60 Hz) for use by onsite building power demands or for export to the electric grid. This power conditioning is achieved with DC/AC inverters and is a critical component of any stationary SOFC power system. The fuel cell-CHP system necessarily requires other components too such as an air filter, flow manifolds, valves and orifices, controllers, sensors, and piping to deliver fuel and air to the stack, and remove waste gases, excess heat, and electricity. Due to the high operating temperature, selecting suitable materials and insulation for components such as pipes and valves are key to ensuring the thermal integrity of the system.

The above conceptual design is an example of system configurations intended for residential and commercial building applications in the 1–400 kW range. In larger systems (*e.g.*, >200kW) micro-turbines can also be integrated into the

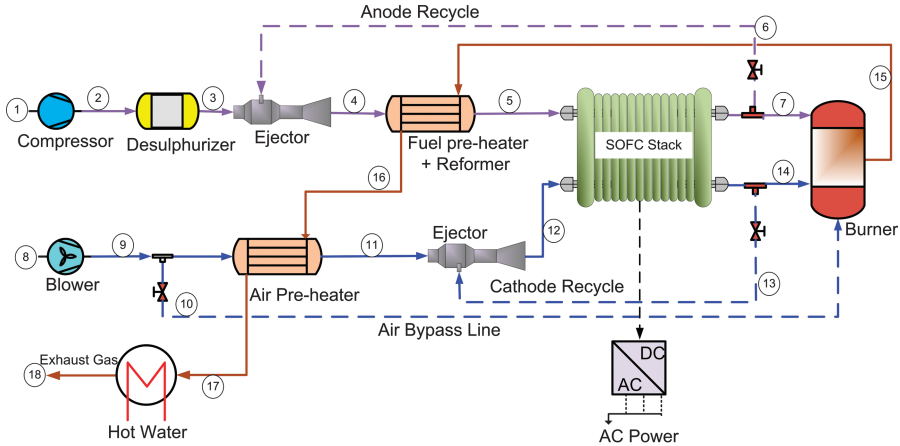


**Figure 12.7** Flowsheet for SOFC-CHP system employing exhaust gas recycle concepts.

system for producing more power and consequently increasing the overall system efficiency. The coupling between gas turbine and SOFC can be done either indirectly or directly.<sup>42</sup> The simplest fuel cell/gas turbine integration consists of a coupling of the two components by a heat exchanger (indirect connection). In this condition, the SOFC exhaust heats compressed air in the micro gas turbine recuperator. The anode and cathode gas preheating can also be done with heat from the gas turbine exhaust gas as well as the burner exhaust flow streams. When the SOFC and the gas turbine are coupled indirectly (by a heat exchanger), TERs of in the range of 0.4 to 0.5 are realizable at SOFC operating temperatures between 950 and 1000 °C.<sup>42</sup>

Direct coupling of SOFC and gas turbine is typically accomplished by operating the SOFC system at pressures above 4 bar (and as high as 20 bar) and directing the exhaust from the tail-gas burner directly into a gas turbine. Direct integration configurations have been explored for both natural gas and coal gasification systems and offer electrical efficiencies of up to 70%<sup>42</sup> Further discussion on integrated SOFC-gas turbine cycles is provided in Chapter 13.

### 12.3.2 SOFC System Description for CCHP (Tri-generation)

The waste heat available in an SOFC system can be utilized to produce cooling through a thermally activated cooling technology. Figure 12.8 illustrates an SOFC system integrated with an absorption chiller and hot water heat exchanger to produce ac power, chilled water, and hot water. The high temperature burner exhaust gas can be utilized to drive a single-, double-, or triple-effect absorption chiller. If a single-effect chiller is integrated with the SOFC system, then the high-grade heat exiting the burner is first used to provide the thermal energy for fuel preheat and pre-reforming and to preheat

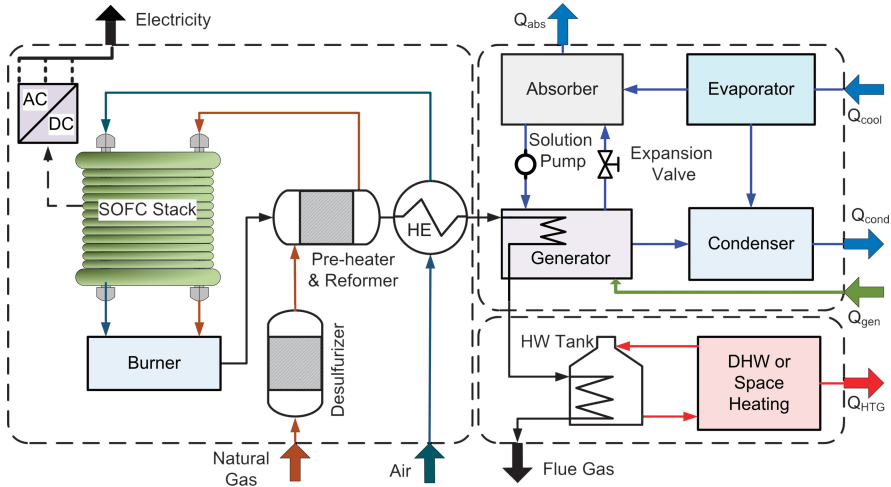


**Figure 12.8** Flowsheet for SOFC-CCHP system integrated with an absorption chiller.

the cathode inlet air before waste heat is recovered in the generator section of the chiller as shown in Figure 12.8. Within the generator, the SOFC exhaust gas heats the refrigerant-absorbent mixture,<sup>‡</sup> resulting in a mixture separation of refrigerant vapour and a strong absorbent liquid solution. The strong liquid solution is led to the absorber where it mixes again with the refrigerant vapour generated in the evaporator. The refrigerant vapour is absorbed into the liquid solution in an exothermic process, where the resulting weak solution is pumped backed into the generator. The evaporator and condenser portions of the absorption chiller operate in the same manner as any vapour-compression system, and thus, heat rejected from both the condenser ( $Q_{cond}$ ) and absorber ( $Q_{abs}$ ) could be recovered for DHW or space heating purposes. Most often the heat is rejected via a cooling tower.

Double- and triple-effect absorption chillers require a higher source temperature and thus, such systems could be integrated with an SOFC system by utilizing the burner tail-gas directly in the generator. Alternatively, steam could be generated in a waste heat recovery boiler that is supplied with high-quality heat from the SOFC exhaust gas and sent to the generator of the chiller.<sup>43</sup>

The appropriate selection and integration of components in a fuel cell-CCHP system depends on numerous parameters such as the system size, load demands, operating strategy, utility energy pricing, climate, and the fuel infrastructure in the building zone. They also change depending on the proposed application. For example, the system can be implemented as either a co-generation system (to produce heat and power demand),<sup>36</sup> or as a

<sup>‡</sup>Typically mixtures of either Li/Br or ammonia-water are employed depending on the required refrigeration temperature.

polygeneration system producing cooling, heat, and power, or heat, hydrogen (or other fuel) and power.<sup>44–46</sup> Although currently many experimental and numerical studies have been conducted on fuel cell stacks in order to develop a more durable and highly efficient power module, only a few practical fuel cell-CHP systems have been developed. As SOFC technology is still in its relative infancy, many aspects of these systems are currently under investigation worldwide. Part of the research focuses on integrating the fuel cell in a system that is both efficient and economically attractive. Because of the emerging systems paradigms related to co- or poly-generation concepts and the interest in alternative fuel feedstocks (*e.g.*, biomass, biogas),<sup>47</sup> integrated system design has become a critical focus for enabling energy conversion systems congruent with forward-looking sustainable development. Furthermore, when these challenges are considered with the great variety of potential CHP/CCHP applications (many of which are unique or require custom DG solutions), identification of optimal system configurations and dispatch strategies are neither trivial nor obvious.

## 12.4 Modelling Approaches: Cell to System

Modelling approaches for application of SOFC-CHP/CCHP systems in commercial buildings depend largely on the purpose of the model. To enable application studies of the effectiveness of fuel cell CHP systems requires annual building energy demand profiles, CHP system models for simulation, utility energy rate structures, dispatch and control models with embedded operating strategies, and economic models for capital and operating cost estimation. Figure 12.9 depicts a model framework for modelling and simulation of DERs that are integrated with building electrical and HVAC energy systems. This structure consists of input parameter data, real-time sensor data, component and system models, decision and logic controllers, and performance analysis tasks. Input data includes weather, building construction characteristics, and costs that are utilized for design and simulation activities. Real-time data is employed to adjust demand profiles, operating strategies, and dispatch control of the various DERs. Thermodynamic component and system models are required to simulate a heterogeneous array of DG technologies. Cost models together with the overall thermodynamic system model are used for the purposes of establishing an optimal system design of the power system performance over a range of load conditions. The generated building loads are employed in a simulation of the energy system technologies dispatched to serve building energy demands. The system simulator computes instantaneous and time-averaged efficiency, economic, and environmental performance. Feedback between the distributed energy system design, operating strategy, and simulation results is necessary to assess ‘optimal’ application design and supervisory control schemes.

Integrated system modelling is typically carried out by dividing the system into subsystems and subcomponents, as implied in Figure 12.10. Figure 12.10

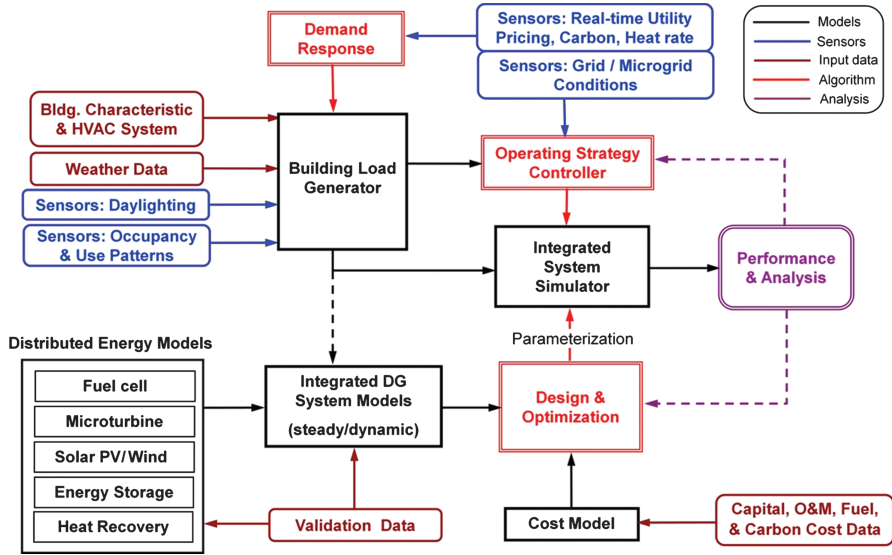


Figure 12.9 Integrated CHP-building model information flow schematic.

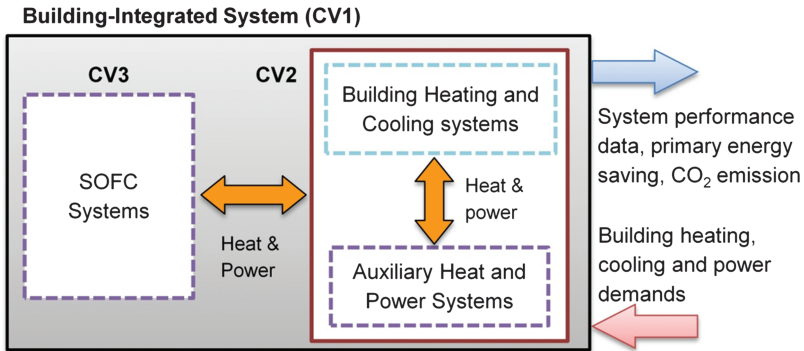


Figure 12.10 Modelling control volume schematic of building-integrated SOFC-CHP system.

shows a simplified view of a building-integrated fuel cell-CCHP system, designated as control volume 1 (CV1), that interfaces with the building energy demands. The overall system may be sub-divided into two primary subsystems: the building CCHP energy systems (CV2), and the SOFC power generator (CV3). CV2 comprises all of the CCHP system components except the SOFC system (*i.e.*, stack, BoP components including heat recovery, and power conditioning which are included in CV3). When the main objective is the conceptual design of the fuel cell system (*i.e.*, CV3), a stand-alone model of this sub-system suffices. Numerous modelling approaches that vary in fidelity from simple black box models to detailed, multi-dimensional models that have a primarily technical focus can be employed for system design and simulation.

Alternatively, model development can be based on either high-level technical or economic assessments of the whole system (*i.e.*, the level of CV1) (Figure 12.10).

Chapters 9, 13 and 14 provide substantial detail on modelling approaches for SOFC cells and systems. Thus, only a high-level overview of system and stack modelling approaches is given here with an emphasis on steady-state performance prediction of SOFC-CCHP systems. Additionally, given the emphasis on application of CCHP systems, approaches for modelling and performance estimation of the heat recovery equipment and building energy systems are summarized in this section. Approaches for system-level design and performance modelling are also provided, where the methods often used for this purpose rely on black or grey box techniques. SOFC cell/stack model formulations whose performance characteristics are semi-empirical are highlighted next. The section concludes with modelling techniques for system optimization.

## 12.4.1 System-level Modelling and Performance Estimation

### 12.4.1.1 General Modelling Overview

System-level models are typically a collection of component models that are integrated such that input and output variables are exchanged between components and whose performance metrics may be interrelated. The mathematical description of the system is formulated in terms of governing equations that are established from: (1) interface and boundary conditions, (2) conservation laws, (3) property and kinetic relations, and (4) performance characteristics of the components. The mass and energy balances written for each component in the system generally follow the form:

$$\text{Mass : } \frac{dm_{cv}}{dt} = \sum_i \dot{m}_i - \sum_e \dot{m}_e \quad (1)$$

$$\text{Energy : } \frac{dE_{cv}}{dt} = \dot{Q}_{cv} - \dot{W}_{cv} + \sum_i \dot{m}_i \left( h_i + \frac{\bar{V}^2}{2} + gz_i \right) - \sum_e \dot{m}_e \left( h_e + \frac{\bar{V}^2}{2} + gz_e \right) \quad (2)$$

where  $m$ ,  $\dot{m}$ ,  $t$ ,  $E$ ,  $\dot{Q}$ ,  $\dot{W}$ ,  $V$ ,  $h$ ,  $g$ ,  $z$  are mass ( $m$ ), mass flow rate ( $\dot{m}$ ), time ( $t$ ), energy ( $E$ ), heat transfer rate ( $\dot{Q}$ ), power ( $\dot{W}$ ), velocity ( $V$ ), enthalpy ( $h$ ), gravitational acceleration ( $g$ ) and elevation ( $z$ ), respectively. The subscripts refer to device inlet  $i$ , outlet  $e$ , and the overall component control volume  $CV$ . Examples of device performance characteristics include fan/blower, compressor/expander, and power-conditioning efficiencies, fuel-cell polarization curves, and the effectiveness of process heat-exchangers within the system. The equations for mass and energy balances, property relationships and performance characteristics form a set of nonlinear-coupled equations incorporating design and operating variables and are common to all energy conversion devices.

### 12.4.1.2 Modelling Building Energy Demands, and Heating and Cooling Systems

Modelling of a building-integrated SOFC-CCHP system (*i.e.*, SOFC, CCHP, building HVAC systems, and building envelope) is mainly used to investigate the system benefits in terms of annual CO<sub>2</sub> emission reductions, primary energy savings, economics and overall efficiency performance compared with either utility-supplied energy or competing DG technologies.<sup>45,48,49</sup> The models used for these purposes usually consider the interaction between the building, CCHP system and the environment. The building (*i.e.*, the application) model input data are the building electrical, cooling and heat demands, which are strongly time dependent, as well as the building characteristics (type, location, construction, occupancy, *etc.*). Models may be developed for short- (hours), seasonal (weeks), or annual simulation of the system. Seasonal simulations are typically employed for a particular time of year, for example, to examine when the thermal or electrical demands are above the nominal ranges (*i.e.*, during winter and summer weeks).<sup>50</sup>

Due to the complicated nature of modelling and simulation of integrated energy systems over durations that may amount to 8,760 hours in a year, it is usually impractical to employ high-fidelity models for all sub-systems. Instead, varying fidelity component and sub-system models are integrated and employed in a fashion that largely depends on factors which relate to both the suitability (*i.e.*, flexibility, capability, availability, cost, *etc.*) of the various software platforms and the individual preferences of the modellers themselves. Currently, there are several commercial software options such as EnergyPlus<sup>24</sup>, ESP-r<sup>51</sup>, BeOpt<sup>52</sup> and TRNSYS<sup>27</sup> whose purpose is to generate the energy and water demand profiles in various building types (*e.g.*, see Figure 12.4(a-d)), as well as provide the means for simulating the various forms of energy supply from onsite renewable and distributed resources. Specifically, these simulation tools can model building heating, cooling, electrical, water usage, onsite DG systems and other energy flows. The models used in these tools are commonly based on quasi-steady state performance characteristics with simple approximations for transient behaviour. To simulate a building-integrated SOFC-CCHP system, it is necessary to develop simplified steady-state or dynamic models for the SOFC sub-system (CV3) since it is not typically available in standard software library components. This approach is commonly used in the literature and is described further in a subsequent section.

### 12.4.1.3 SOFC System-level Modelling

SOFC system-level models (as opposed to building-integrated models) may be used to establish a conceptual process design, for cost and performance analysis (in both steady-state and transient conditions), and/or for optimization purposes. These models can also be employed to evaluate the effect of some detailed parameters of the SOFC system such as fuel utilization, operating voltage, and cell operating temperature, or they can also be used to calculate the spatial distribution of one or more specific parameters inside a plant component (*e.g.*, the temperature distribution along SOFC channels).

Zero-dimensional thermodynamic models are typically employed for high-level system design and analysis purposes. In this thermodynamic modelling approach, the system can be viewed in terms of the input/output and transfer characteristics without following the details of the internal processes. This modelling approach can be sub-divided into two categories: the so-called ‘grey box’ and ‘black box’ approaches which differ from one another primarily on the basis of information resolution with respect to the system outputs. For example, in a grey box approach, given inputs of fuel type, flow, and ambient conditions, only bulk system performance, such as net power, efficiency, waste heat available, etc., is estimated. More detailed information such as stack temperature, cell temperature gradients, gas composition, *etc.* are not typically available. In black box modelling, bulk system performance estimation is accomplished by individual modelling of the entire set of integrated components which make up the system (*i.e.*, CV3-3 through CV3-7) as shown in Figure 12.11. The grey box modelling approach has been followed in various international projects focused on developing simulation tools for the conceptual design, analysis, and environmental and economic evaluation of CHP systems employing fuel cells and internal combustion (IC) engines in stationary building applications. For example, the modelling strategy employed in the Annex 42 project implemented grey box CHP (fuel cell and IC engines) models to existing whole-building simulation programs such as EnergyPlus and TRNSYS.<sup>53</sup> However, to solve the set of equations governed by the conservation laws (mass and energy), the performance characteristics (*e.g.*, electric efficiency and airflow versus net system power output) of the fuel cell module must be inputted. Performance curves may be approximated as simple polynomial expressions where the constant coefficients are established from either experimental data or predicted data derived from higher fidelity cell, stack, or fuel cell system models.

Modelling SOFC-CHP systems using methods consistent with black box techniques are generally more common in the technical literature. This approach involves building a model by establishing a control volume around each plant component (or set of components) and applying conservation equations, property and kinetics relations, and performance characteristics in

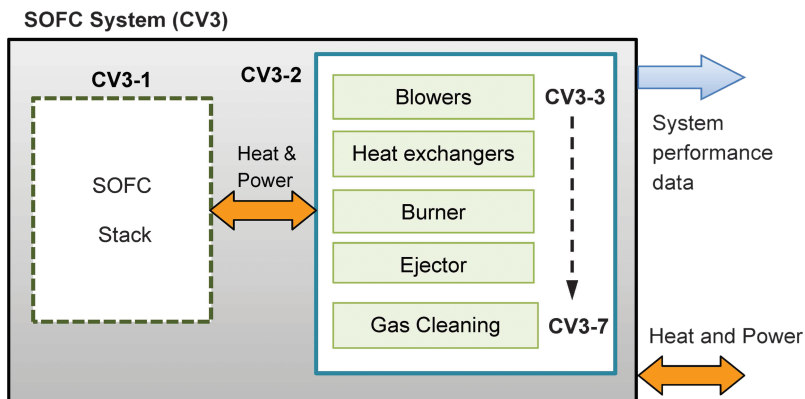


**Figure 12.11** Modelling control volume schematic of SOFC and balance-of-plant.

order to generate a system of equations which characterize the physicochemical processes occurring within. One particular advantage of this modelling methodology is that it enables varying levels of model fidelity to be applied to different devices. For example, SOFC stack performance estimation can be accomplished with much higher fidelity using one- or two-dimensional models, thereby enabling cell temperature profiles and gradients, reactant utilizations, *etc.* to be resolved. SOFC system modelling and simulation can be accomplished using commercial tools such as Aspen Plus<sup>54</sup>, gPROMS<sup>55</sup>, and TRNSYS that have libraries for the standard (*i.e.*, BOP) components and custom models for that represent the SOFC stack and other unconventional devices. It is also not uncommon to develop system level models without using the commercial chemical engineering software platforms. Such approaches, for example, have been used by Braun *et al.*<sup>23</sup> and Kazempoor *et al.*<sup>39</sup> to develop system models in EES software environment.<sup>56</sup> Black box steady-state and dynamic modelling approaches for various BOP components have been provided in many studies, the details of which can be found in references.<sup>23,29,47,49</sup>

#### 12.4.1.4 CCHP System Performance Metrics

Numerous system efficiencies are utilized when evaluating performance of SOFC-CCHP systems. For CCHP systems employing thermally activated cooling technologies, the absorption chiller is the most common device that is integrated with prime movers. The coefficient of performance (*COP*) is a performance metric for conventional refrigeration and absorption chiller systems and is quantified by the useful thermal energy produced divided by the energy supplied to the system as given below,

$$COP_{\text{abs}} = \frac{\dot{Q}_{\text{cool}}}{\dot{E}_{\text{in}}} \quad (3)$$

where  $\dot{Q}_{\text{cool}}$  is the cooling developed by the chiller in the form of chilled water and  $\dot{E}_{\text{in}}$  is the sum of the thermal energy and auxiliary power supplied to the chiller. The nominal COPs for single-, double-, and triple-effect absorption chillers are about 0.7, 1.2, and 1.5, respectively.<sup>19</sup> At the system level, several useful efficiency metrics are defined as follows,

$$\text{Net system electric efficiency : } \eta_{\text{e}}^{\text{sys}} = \frac{P_{\text{AC,net}}}{(\dot{m}_{\text{fuel}} \cdot LHV_{\text{fuel}})_{\text{system inlet}}} \quad (4)$$

$$\text{System CHP efficiency : } \eta_{\text{CHP}} = \frac{P_{\text{AC,net}} + \dot{Q}_{\text{HR}}}{(\dot{m}_{\text{fuel}} \cdot LHV_{\text{fuel}})_{\text{system inlet}}} \quad (5)$$

$$\text{System CCHP efficiency : } \eta_{\text{CCHP}} = \frac{P_{\text{AC,net}} + \dot{Q}_{\text{HR}} + \dot{Q}_{\text{gen}}}{(\dot{m}_{\text{fuel}} \cdot LHV_{\text{fuel}})_{\text{system inlet}}} \quad (6)$$

where  $P_{\text{AC,net}}$  is the net system AC power,  $\dot{Q}_{\text{HR}}$  is the amount of thermal energy from the SOFC system exhaust gas that is recovered and exported for heating

purposes,  $\dot{Q}_{\text{gen}}$  is the thermal energy extracted from the SOFC exhaust gas and supplied to the generator section of an absorption chiller (for example),  $\dot{m}_{\text{fuel}}$  is the mass flow rate of fuel supplied to the CCHP system, and  $LHV_{\text{fuel}}$  is the fuel lower heating value. The heating and cooling efficiencies are measures of the thermal energy recovered from the system relative to the fuel energy input,

$$\text{System heating efficiency : } \eta_{\text{HTG}} = \frac{\dot{Q}_{\text{HR}}}{(\dot{m}_{\text{fuel}} \cdot LHV_{\text{fuel}})_{\text{system inlet}}} \quad (7)$$

$$\text{System cooling efficiency : } \eta_{\text{cool}} = \frac{\dot{Q}_{\text{gen}}}{(\dot{m}_{\text{fuel}} \cdot LHV_{\text{fuel}})_{\text{system inlet}}} \quad (8)$$

Calculating the sensible energy recovered (*i.e.*,  $\dot{Q}_{\text{HR}}$  or  $\dot{Q}_{\text{gen}}$ ) is a straightforward thermodynamic evaluation of the change in enthalpy of the SOFC exhaust gas. For example, given the SOFC-CHP system presented in Figure 12.7, calculating the rate of heat recovered is given by,

$$\dot{Q}_{\text{HR}} = \dot{m}_{17}(h_{18} - h_{17}) = \dot{m}_{\text{HW}}c_{p,w}(T_{\text{out}} - T_{\text{in}}) \quad (9)$$

where the  $h$ 's are the enthalpy of the SOFC exhaust gas,  $\dot{m}_{\text{HW}}$  is the flow rate of hot water into the heat recovery heat exchanger and  $T_{\text{out}}$  and  $T_{\text{in}}$  are the water outlet and inlet temperatures, respectively. In calculating the amount of heat recovered, the exhaust gas temperature after the heat exchanger needs to be determined and is typically above the dew point temperature of the flue gas. Prediction of the outlet gas temperature can be made once the heat exchanger performance characteristics (*e.g.*, surface area and overall heat transfer coefficient) are known via effectiveness-NTU approaches. SOFC pre-commercial systems under development, such as the Hexis micro-CHP device, allow for condensation in the exhaust gas, thereby increasing the heating efficiency. For CCHP systems employing an absorption chiller, the generator heat exchanger effectiveness must be known.<sup>21,43</sup> Further, when coupling an SOFC device to a thermally driven chiller, heat normally has to be extracted and supplied to the chiller at temperatures of at least 80 °C.<sup>19,57</sup>

Total efficiency or CCHP efficiency of the SOFC-CCHP system is the summation of electrical (AC), heating, and cooling efficiencies and therefore can also be expressed as,

$$\eta_{\text{CCHP}} = \eta_{\text{el}}^{\text{sys}} + \eta_{\text{HTG}} + \eta_{\text{cool}} \quad (10)$$

and similarly,

$$\eta_{\text{CHP}} = \eta_{\text{net,el}} + \eta_{\text{HTG}} \quad (11)$$

It should be noted that although one might be inclined to employ a CCHP system efficiency that uses  $\dot{Q}_{\text{cool}}$  (see Eq. 3) as opposed to  $\dot{Q}_{\text{gen}}$  this could result in an overall system efficiency greater than 100% since double- and triple-effect absorption chiller COPs are greater than one. The proper efficiency expression only allows the total thermal energy extracted from the prime mover

sub-system to be employed. Furthermore, industry efficiency expressions are typically based on the fuel lower heating value (LHV); but when considering CHP and CCHP systems, particularly those that utilize condensing gas heat recovery heat exchangers, a higher heating value (HHV) basis is more appropriate and reflective of the true efficiency potential of the system.

Annual capacity (or load) factors for SOFC-CCHP systems are useful performance indices considering stationary building applications. These factors are represented on electric and thermal energy-supplied bases. As given by Eq. (12), the system electric capacity factor  $CF_e$  is defined to mean the ratio of the electricity produced by the CHP system for a given time interval over the electricity that would have been produced if the plant operated 100% of the time at its rated capacity,

$$CF_e = \frac{(\text{kWh electricity supplied by CCHP system})}{(\text{Max. kWh electricity supplied at 100\% rated power})} = \frac{E_{el,actual}}{E_{el,max}} \quad (12)$$

Similarly, expressions for heating and cooling capacity factors can be written as,

$$CF_h = \frac{(\text{kWh heating supplied by CCHP system})}{(\text{Max. kWh heating supplied at 100\% rated power})} = \frac{E_{h,actual}}{E_{h,max}} \quad (13)$$

$$CF_c = \frac{(\text{kWh cooling supplied by CCHP system})}{(\text{Max. kWh cooling supplied at 100\% rated power})} = \frac{E_{c,actual}}{E_{c,max}} \quad (14)$$

## 12.4.2 Cell/Stack Modelling for SOFC System Simulation

Fuel cell models can be developed to meet a wide range of objectives. Achieving diverse objectives usually requires that the models incorporate significantly different levels of sophistication. For systems design and performance, the level of modelling detail required for most system components is limited to overall mass and energy balances and incorporation of component performance characteristics. However, the relative infancy of fuel cell technology requires that simulation of the fuel cell stack component be driven by a more detailed cell-level model. One-, two-, or three-dimensional cell-level models may be written depending on the requirements of the user. Two- and three-dimensional modelling are generally concerned with cell and stack design efforts. The design of SOFC stacks benefits from models that can predict gas flows through inlet and exhaust manifolds, flow distribution into multiple channel networks, and in-channel reaction chemistry and transport phenomena. Understanding and controlling thermal variations within the stack is another important stack-level design consideration. Models that focus on transport and chemistry at the microscale provide great value in assisting the optimization of MEA structures, but are not needed for stack simulation.<sup>38</sup> Detailed cell and stack models are outside the scope of this chapter, but some approaches are given in references.<sup>29,38,40,58-60</sup>

### 12.4.2.1 Simplified Cell-level Modelling

Relatively low-fidelity models of the fuel cell stack (see CV3-1 in Figure 12.11) can be constructed readily from modelling single-cells and then extrapolating single-cell performance to be representative of an SOFC stack of  $N$  cells. Reactant gas supply is assumed to be uniformly distributed among the cells within the cell-stack and among the channels within each repeat unit. This representation can be readily constructed as quantities such as stack voltage and stack power are scaled versions of single-cell voltage and power. Thus, in this manner, a single-cell model forms the heart of an SOFC stack model. The method is implemented by the coupling of mass and energy balances (written over anode/cathode inlets and outlets) with a polarization curve whose operating point is specified through a set of fixed operating parameters (*e.g.*, reactant utilization, cell temperature, *etc.*). Both zero- and multi-dimensional modelling can be applied with this general methodology. The simplest approach is a zero-dimensional (0-D) model of the cell which serves as a lumped, single-node thermodynamic representation that accounts for internal reforming and water-gas shift equilibrium, electrochemical polarizations and the associated heat generation, and mass transfer from cathode to anode (via cell reactions) within a single-cell repeat unit.<sup>4,61</sup>

A model with higher fidelity can be achieved by moving to a one-dimensional (1-D) representation of the cell, which results in a so-called channel model. One-dimensional cells models can be utilized to great effect for system studies. Depending upon the intended application and available computation resources, full stacks of cells can be represented as arrays of channels where, as noted before, each channel in the stack may be assumed to have identical behaviour.<sup>34,35</sup> These so-called channel models enable 1-D steady-state and dynamic cell behaviours to be simulated and are powerful tools for integration with system-level component models. These models still rely on performance extrapolation and thus, the models must be experimentally validated or calibrated for simulation and optimization purposes. In practice, of course, each channel performs differently depending upon the stack design (flow manifolds, thermal insulation, *etc.*).<sup>38</sup> However, the differences may not be meaningful in terms of errors in stack voltage and power prediction.<sup>62</sup> The 1-D modelling approach has been successfully used for the SOFC system studies using different cell geometries (*i.e.*, planar, tubular, delta, segmented-in-series, *etc.*).<sup>23,29,47</sup> Further discussion of one-dimensional channel-type cell models is given in references.<sup>34,38,39,58</sup>

In both zero- and one-dimensional approaches, the cell model is comprised of three compartments – the anode, the cathode and the electrolyte. Figure 12.16 depicts the model architecture of a 0-D, single-cell where the temperature across the cathode is typically specified, and  $T_{\text{cell}}$  and  $P_{\text{cell}}$  are the temperature and pressure at which the electrochemistry functions are evaluated. Mass balances are written individually for the anode and the cathode compartments taking into account that the consumption of  $\text{H}_2$  in the anode and  $\text{O}_2$  in the cathode is governed by Faraday's law and is proportional

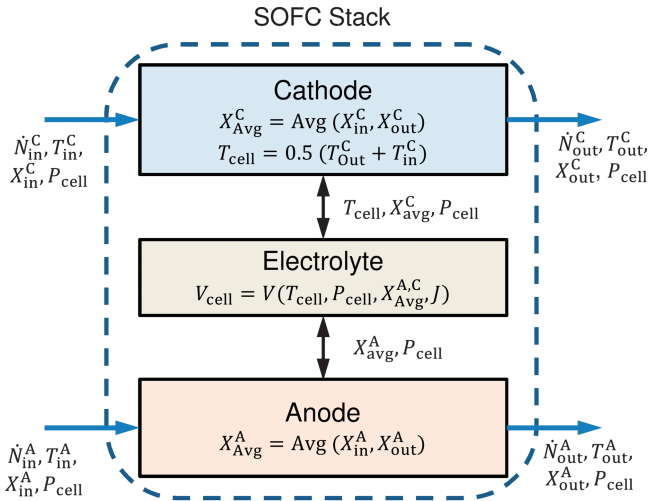


**Figure 12.12** SOFC stack model overview.

to the current density. As given in the Figure 12.12,  $\dot{N}^C$  and  $\dot{N}^A$  are the molar flow of species into or out of the cathode and anode, respectively. The terms  $X^C$  and  $X^A$  are the molar fractions of species at the cathode and anode inlets and outlets, respectively,  $T$  is either the cathode gas, anode gas, or cell temperature, and  $P_{cell}$  is the pressure. This approach presumes that hydrocarbons and carbon monoxide are not electrochemically active but are consumed rather through reforming and water-gas shift (WGS) reactions. The produced  $H_2$  then is the only participant in electrochemical oxidation at the triple-phase boundary and the WGS and reforming reactions are taken to be in equilibrium at the anode outlet. Mass balance equations must account for compounds consumed/produced due to the WGS, reforming and electrochemical reactions. Quantities such as fuel utilization and  $O_2$ -stoichiometry can either be calculated from the mass-balance equation framework or specified as input parameters.

An overall system energy balance (see Eq. (2)) accounts for enthalpy-flows and external heat losses from the stack. The total enthalpy-flow into the system has two components: the anode inlet flow and the cathode inlet flow. Similarly, the enthalpy-flow out of the system has the anode outlet and cathode outlet flow components. When a load is applied, the lumped system produces power and rejects thermal energy to both the surroundings and the cathode cooling air stream.

The electrochemical model that translates the charge-transfer equations into a cell voltage (and ultimately into a cell voltage-current performance map) is summarized below:

$$V_{cell} = V_{Nernst} - \eta_{Ohmic} - \eta_{Act} - \eta_{Conc} \tag{15}$$

$$V_{\text{Nernst}} = E_0 + \frac{R_u T}{n_e F} \ln \left( \frac{P_{\text{H}_2} P_{\text{O}_2}^{0.5}}{P_{\text{H}_2\text{O}}} \right) \quad (16)$$

$$\eta_{\text{Ohmic}} = J \cdot R \quad (17)$$

$$\eta_{\text{Act}} = \frac{2R_u T}{n_e F} \sinh^{-1} \left( \frac{J}{2J_{0, \text{Anode}}} \right) + \frac{2R_u T}{n_e F} \sinh^{-1} \left( \frac{J}{2J_{0, \text{Cathode}}} \right) \quad (18)$$

$$\begin{aligned} \eta_{\text{Conc}} &= \eta_{\text{act}}^{\text{anode}} + \eta_{\text{act}}^{\text{cathode}} \\ &= \frac{R_u T}{n_e F} \sinh^{-1} \left( \frac{1}{1 - J/J_{L, \text{O}_2}} \right) + \frac{R_u T}{n_e F} \sinh^{-1} \left( \frac{1 - J/J_{L, \text{H}_2}}{1 - J/J_{L, \text{H}_2\text{O}}} \right) \end{aligned} \quad (19)$$

where  $E_0$ ,  $V_{\text{Nernst}}$ ,  $R$ ,  $P_i$ ,  $R_u$ ,  $n_e$ ,  $F$ ,  $J_0$ ,  $J_L$  are the standard equilibrium potential ( $E_0$ ), the Nernst cell potential ( $V_{\text{Nernst}}$ ), specific ohmic resistance ( $R$ ), partial pressure of gas species  $i$  ( $P_i$ ), universal gas constant ( $R_u$  in  $\text{J k}^{-1} \text{mol}^{-1}$ ), number of electrons transferred per electrochemical reaction ( $n_e = 2$ ), the Faraday constant ( $F = 96485 \text{ C mol}^{-1}$ ), exchange current density ( $J_0$  in  $\text{Am}^{-2}$ ) and limiting current density ( $J_L$  in  $\text{Am}^{-2}$ ), respectively. In a lumped model, the fuel cell operating conditions ( $T$ ,  $P_i$ ) are then based on the average cathode gas temperature and the average gas compositions of the inlet and outlet fuel and air streams. These averaged quantities are employed in the electrochemical model equation set given by Eqs. (15)–(19).

Eqs. (15)–(19) are coupled, non-linear functions of the temperature and gas species inside the stack. Therefore, the set of governing equations can only be solved iteratively.<sup>60</sup> The main limitation with the above approach is that because the channel gas composition and temperature variations are neglected, different results are obtained depending on if the inlet, outlet or average values of these parameters are employed for the calculations. Bove *et al.*<sup>60</sup> have examined the effect of considering the three different reference values (*i.e.*, inlet, outlet, or average) on the V-J cell polarization curve using a black box SOFC model. Their results show that the effect of fuel consumption along the gas channel cannot be estimated if the inlet gas composition is used. The cell voltage may also be underestimated if the output gas composition is considered into the calculation. A good agreement between the experimental and numerical data can be obtained by considering average values between inlet and outlet streams, however, the choice of utilizing average or outlet compositional values depends to some extent on how well the polarization characteristic can be fitted to the data. The coupled nature of the governing equations typically requires an iterative numerical solution algorithm. When using the average values, the iteration can be started by predicting the outlet gas compositions and outlet temperature of the flow streams. The set of equations from the electrochemical model (Eqs. (1), (2), (15)–(19)) can then be solved for the operational voltage. With knowledge of the cell voltage, the mass and energy balances equations can be solved simultaneously for predicting the outlet parameters, until convergence is obtained.

The 0-D model input/output and parameters are summarized in Table 12.2. The inputs to the cell model are average cell current density (or cell voltage),

**Table 12.2** SOFC model inputs, outputs, and parameters.

<i>Inputs</i>	<i>Outputs</i>	<i>Model Parameters</i>
Avg. current density, $J_{\text{cell}}$ (or $V_{\text{cell}}$ )	Cell voltage, $V_{\text{cell}}$ (or $J_{\text{cell}}$ )	V-I characteristic ( $R, J_0, J_L$ )
Inlet gas temperatures, $T_{\text{in}}^C, T_{\text{in}}^A$	Cell power, $P_{\text{DC}}$	Cell geometry: Area
Reactant gas temperature rise (DT)	Fuel flow, $\dot{N}_{\text{in}}^A$ (or $U_f$ )	
Cell temp., $T_{\text{cell}}$ (or $\dot{N}_{\text{in}}^A$ or $DT_{\text{air}}$ )	Air flow, $\dot{N}_{\text{in}}^C$	
Fuel utilization, $U_f$ (or $\dot{N}_{\text{in}}^A$ )	Outlet fuel and air temps, $T_{\text{out}}^C, T_{\text{out}}^A$	
Inlet gas compositions ( $X_i$ )		

air-to-fuel ratio, inlet fuel and air temperatures, anode and cathode gas temperature rises, fuel utilization (or fuel flow), and inlet compositions. Fixed parameters (*i.e.*, geometry and performance characteristics) are the polarization curve constants, and cell area. The outputs of the model are cell voltage (or current density), power, efficiency, air flow, fuel flow (or fuel utilization,  $U_f$ ) and outlet temperature of the fuel and air streams.

Although this modelling approach is usually sufficient for the preliminary design and concept studies of SOFC-CHP systems, the method is only concerned with the input and output values and cannot generate any information about the distributed parameters inside the stack.

The successful design and analysis of an SOFC system generally requires a more detailed model of the components especially the cell-stack. For example, the local temperature gradient (and local solid temperatures, fuel depletion zones, *etc.*), as well the local steam to carbon ratio (SC) are important parameters which must be maintained within specified limits in order to ensure no harmful damage occurs. Even for a well-designed SOFC system, these parameters may exceed their allowable range. The maximum allowable temperature gradient and increase are about  $15 \text{ K cm}^{-1}$  and  $150 \text{ K}$ , respectively,  $\text{SC} > 2$  is also necessary for protecting the cell from any carbon deposition.<sup>63</sup> Thus, for model objectives intent on establishing viable SOFC system designs and performance prediction, a higher-fidelity model of the SOFC stack is necessary in order to resolve the distributed functions of temperature, current density, composition, *etc.*

#### 12.4.2.2 Simplified Stack Modelling

The use of multi-dimensional SOFC stack modelling tools is generally too computationally intensive and inefficient for system design, simulation and optimization purposes. One exception can be in designs where the SOFC power module is tightly thermally integrated and, as a result, boundary and input conditions to the various unit operations within the system are coupled due to the proximity and packaging geometry of system components. In such cases, large-scale computational fluid dynamics software augmented with special

purpose software for cell electrochemistry may be employed for system simulation.<sup>40,64</sup> However, the more common approach is to extend the 1-D cell model to represent stack performance by considering appropriate assumptions and losses. A 1-D model usually relies on several assumptions such as uniform distribution of feed gases to each individual cell and channel, adiabatic boundaries at the cells or channels surrounding area, isopotential surfaces at each cell, *etc.* Even for a well-designed stack, these assumptions might not be valid and the associated losses must be considered in the calculation. In addition, experimental<sup>65-67</sup> and numerical studies<sup>65,68,69</sup> show that the voltage versus current density for SOFC stacks is significantly below the results presented for button- and single-cell configurations. Therefore, it is likely that besides the major cell overpotentials (*i.e.*, ohmic, activation and concentration), there are other significant losses that also must be considered to extend a 1-D cell model be more representative of stack performance estimation. Other cell polarizations may be related to an increased overall ohmic resistance of the entire stack due to: (1) the contact resistances at the interfaces between the electrodes and the electrolyte, (2) contact resistance between the electrodes and the current collectors, and (3) the resistance of stack current collection and associated wiring. The small contact area between ceramic components and resistive phases or potential barriers at the cell interfaces are two main contributions of the overall cell contact resistance. Besides the contact resistance, long in-plane conduction paths inside the electrodes can also be counted as a source of additional ohmic losses (if true, such a resistance could negate the appropriateness of isopotential electrode surface assumptions in the cell model). There are several parameters such as mechanical load, and both the temperature and size of cell components which can affect the overall cell contact and in-plane resistances.<sup>66</sup> In some recently reported experimental studies, 60% (or even more) of the overall stack voltage losses are estimated to be attributable to the above contact resistances.<sup>70</sup>

A modification to the ohmic polarization term given by Eq. (17) can then be made as follows,

$$\eta_{\text{Ohmic}} = J (R_{\text{PEN}} + R_{\text{IC}} + R_{\text{contact}}) \quad (20)$$

where  $R_{\text{PEN}}$ ,  $R_{\text{IC}}$ , and  $R_{\text{contact}}$  are the ohmic resistance of the PEN structure, interconnectors, and the resistance due to the contact between the cell components, respectively.

Evaluation of the pressure losses in the stack components are also a challenge in extrapolating cell performance prediction to full stack results. As mentioned before, the blower, pump, and compressor must be used to overcome the system pressure losses and are major contributors to part of the SOFC system auxiliary power consumption. Thus, the correct evaluation of the pressure losses in each individual component is an essential part of the system modelling. With 0- and 1-D reduced order models, the pressure losses in the fuel and air manifolds as well as the feed headers cannot generally be calculated. A generic model which accounts for the pressure losses in the stack certainly has its

limitations and shortcomings, as SOFC stack analysis is very much dependent on the actual design. A number of studies concerning experimental and mathematical modelling have been presented for calculation of the pressure losses in SOFC stacks.<sup>71,72</sup> A general model which solves mass and momentum equations to predict pressure drop and flow uniformity within individual channels based on dimensionless groups has been developed in reference.<sup>72</sup>

### 12.4.3 System Optimization Using Techno-economic Model Formulations

Techno-economic modelling is a method whereby the technical performance characteristics of an energy conversion system translate into economic outcomes, such as the levelized cost of electricity, net present value, or other life cycle cost metrics. One objective of SOFC-CCHP system design optimization is to judiciously account for the competing objectives of capital and operating cost minimization subject to both system design and application constraints. The importance of techno-economic models is that they enable quantification of the economic benefits of CCHP system operation in a given application. Fuel-cell system performance characteristics are largely driven by cell-stack design parameters such as cell voltage, fuel utilization, operating temperature and cathode gas temperature rise. Further, the design operating point strongly influences the capital costs of the major system hardware components, such as the SOFC stack, fuel reformer, airblower and preheater, and heat recovery equipment. The operating costs are primarily associated with fuel consumption (or efficiency). Quantitatively understanding and predicting the cost–benefit trade-offs is the objective of techno-economic modelling and optimization.

Minimizing the SOFC-CCHP system life cycle costs (LCCs) is often employed as one basis for system optimization. For distributed CCHP applications, the LCC may be expressed in terms of an effective levelized cost of electricity (LCOE) where waste heat recovery for heating and cooling purposes provides value and is incorporated into the *LCOE* calculations. Cost models incorporate the forecasts for manufacturing costs of the SOFC and BOP components. The models consider capital and maintenance costs, utility energy prices (grid electricity and natural gas), interest and energy inflation rates, and system efficiency.

In a distributed CCHP application, the LCOE can be expressed as,

$$\begin{aligned}
 LCOE_{CCHP} = & \underbrace{\frac{(CRF \cdot C_{CCHP}^{sys})}{CF_e \cdot A_{plant}}}_{\text{system capital cost}} + \underbrace{\sum MC_j}_{\text{maintenance}} \\
 & + \underbrace{\left( \frac{F_c}{\eta_e^{sys}} \cdot \left[ 1 - CF_h \left( \frac{\eta_{HTG}}{\eta_{B,HS}} \right) - CF_c \left( \frac{\eta_{cool}}{\eta_{B,CS}} \right) \right] \right)}_{\text{Fuel cost - Thermal energy credits}}
 \end{aligned}
 \tag{21}$$

where the first term in this expression is associated with the capital costs, the second term with maintenance costs, and the third term with fuel costs. The capital recovery factor ( $CRF$ ) is defined to mean the ratio of a constant annuity and the present value of receiving that annuity for a specified period of time. The installed capital cost for an SOFC-CCHP system is expressed as  $C_{\text{CCHP}}^{\text{sys}}$  (in \$/kW). The system capacity factors  $CF_e$ ,  $CF_h$ , and  $CF_c$ , have been previously defined (See Eqs. (12) to (14)). In the event that there is system downtime, the expected annual plant availability,  $A_{\text{plant}}$ , will be less than 8760 hours. The levelized annual maintenance cost,  $MC_j$  is the sum of each of the component  $j$  contributions (in \$/kWh). The unit fuel cost is  $F_c$  (e.g., \$/kJ) and  $\eta_{\text{B,HS}}$  and  $\eta_{\text{B,CS}}$  are the building heating and cooling system efficiencies, respectively, which would get displaced by the installation of the CCHP system. Transmission and distribution costs do not factor into the LCOE for on-site power generation.

Detailed capital cost data for SOFC systems is given elsewhere<sup>41,73,74,75</sup> and can be used to generate cost functions that are employed to estimate the first costs, such as in Eq. (21). The LCOE can serve as the basis for an LCC objective function that is minimized to optimize the hardware configuration in a system or to optimally select design parameters within a given system configuration.<sup>41</sup> Optimization of the system configuration for SOFCs has been explored parametrically<sup>39,41</sup> and more recently using mixed-integer linear and nonlinear programming<sup>76,77</sup> including system sizing and optimal dispatch of an SOFC-CHP system for a building application.<sup>57,78</sup> The objective function that is formulated from minimization of the system  $LCC$  is subject to constraints such as mass and energy conservation, property and kinetics relations, and performance characteristics of all hardware within the system. The resulting optimization problem is highly nonlinear and usually involves several independent variables to optimize on.<sup>78</sup>

## 12.5 Evaluation of SOFC Systems in CCHP Applications

### 12.5.1 Micro-CHP

Micro-CHP is the simultaneous generation of heat and power for small-scale building applications such as residential homes and small commercial buildings whose electric power demands are generally lower than 20 kW. The residential energy sector is one potential application for SOFC-CHP systems and is responsible for 22% of the total annual energy consumption in the U.S.<sup>79</sup> with over 69% of that energy consumption being used for low-efficiency space heating (43%), domestic hot water (18%), and air-conditioning (8%).<sup>80</sup> While the residential sector has substantial room for improvements in energy efficiency, it is also one of the most challenging markets to compete in due to the low cost and maintenance, and high durability and efficiency requirements. Despite these requirements, there are substantial potential benefits to

deployment of the technology and numerous SOFC companies are developing systems for residential CHP applications as discussed further in Section 12.6.

Several studies have examined the potential benefits and challenges of grid-connected SOFC-CHP systems in this market sector. Average residential building electrical energy demands vary substantially and depend on the size and building construction of the dwelling, occupancy patterns and geographic location. Average hourly electric demand typically ranges between 0.50 kW and 2.0 kW and thus, studies involving SOFC-based micro-CHP systems are often based on 1 kW size systems.<sup>41,49,81</sup> The operating strategy for micro-CHP systems is dependent on several factors including the annual or seasonal TER of the building and utility energy pricing and net metering plans. In northern European countries, where annual thermal demands are relatively higher than warmer climates, operating strategies for micro-CHP are typically envisioned to be heat-led, although cost optimal operating strategies often involve a combination of heat- and electricity-led load-following modes over the course of a year.<sup>49,82,83</sup>

SOFC-CHP systems that employ some amount of steam methane internal reforming have been predicted to achieve net system electric efficiencies of about 45%-LHV (40%-HHV) at nominal single-cell voltages of around 0.75 V/cell, 85% fuel utilization, and a nominal operating temperature of about 750 °C.<sup>41,23</sup> Total CHP efficiency is estimated to range between 75 and 85%-LHV depending on the SOFC system configuration, heat recovery strategy, and the magnitude of the system heat losses. Higher electric efficiency (above 55%) is possible when operating the SOFC stack at higher cell voltages (*i.e.*, approaching 0.85 V/cell), but this also requires a larger (by as much as 3X) and more costly cell-stack to achieve the same power output. Table 12.3

**Table 12.3** Basic technical characteristics of four key micro-CHP systems synthesized from published literature.

	<i>Internal combustion engine</i>	<i>PEFC</i>	<i>SOFC</i>	<i>Stirling engine</i>
Electrical efficiency (part load, full load)	10%–20%	30%, 26%	45%, 40%	5%, 10%
Overall efficiency (part load, full load)	80%, 85%	80%, 85%	75%, 80%	80%, 90%
Supplementary thermal system efficiency	86%	86%	86%	86%
Minimum operating set point (% of rated power)	20%	20%	20%	20%
Minimum up-time (min)	10	60	60	10
Maximum ramp rate (kW <sub>e</sub> min <sup>-1</sup> )	0.2	0.2	0.05	0.2
Start-up energy consumption (kW <sub>e</sub> , kW <sub>th</sub> )	0.008, 0.5	0.017, 1.6	0.017,2.0	0.008,0.5

provides a comparison of the micro-CHP system technological characteristics that have been synthesized in the literature.<sup>84</sup>

Simulations of 1 kW SOFC micro-CHP systems with about 35%-LHV electric efficiency (95% CHP efficiency) for residential buildings in Europe have been performed operating in a heat-following control strategy to supply hot water for DHW and space heating loads.<sup>49</sup> The authors found that non-renewable primary energy reductions of over 45% could be achieved if the thermal energy output of the fuel cell matched the thermal demands of the building. The capacity factor of the fuel cell was also observed to improve when applied in multi-family housing. The influence of an application in colder climates has also been noted to increase the annual CHP efficiency when in electric load-following modes due to the higher annual water heating demand.<sup>50</sup>

Selection of system size, operating strategy and utility electricity and gas prices are critical parameters in the successful deployment of SOFC micro-CHP systems. Simulation studies of an SOFC-CHP system configured with anode gas recycle can provide broad insights into application considerations as illustrated in Figure 12.6 where the electric power and heat produced are supplied to a prototypical U.S. residence. For example, one such study integrated the aforementioned system with a two-tank (preheat heat exchanger and a standby tank) thermal storage system to supply domestic hot water to serve the energy demands of a household located in Madison, Wisconsin (see Figure 12.4(d)).<sup>34</sup> Capital and maintenance costs for SOFC-CHP systems with electric power capacities of between 1 to 5 kW were estimated and simulations on an annual hourly basis were performed. Installed unit capital costs were based on high volume, mature technology cost projections and ranged from 1500 \$/kW for the 5 kW system to 2450 \$/kW for the 1 kW system in the analysis. The simulation studies are for grid-interconnected systems in which the electric utility acts a peaking plant, providing power to the house when the instantaneous electrical demand cannot be met with the SOFC system. Importantly, maximum system turndown for all systems simulated was 5:1 or 20% of rated electric capacity; thus a 2 kW system, for example, would either have to shut-off or move to a hot standby mode if a load of 400 W was not available. A sample electric-led, load-following operating strategy for a 2 kW SOFC-CHP system is depicted in Figure 12.13(a,b), showing both building load and fuel cell electric power and thermal energy production profiles.

Figure 12.14(a) shows that the SOFC electric capacity factor ( $CF_e$ ) decreases with increasing system size. The electric capacity factor performance of the fuel cell indicates that a 2 kW size solid oxide fuel cell is under-utilized as only 43% of its annual electrical energy production capacity was used. Decreasing the fuel cell system to 1 kW increases the electric capacity factor to 77%. Other methods to increase the fuel cell system electric capacity factor include using an even smaller SOFC system, base-load operation using 'net metering,' employing lead acid batteries, and heat pumping. The heating thermal capacity factor ( $CF_h$ ) of the fuel cell system is also a useful measure and Figure 12.14(a) indicates that a 1 kW SOFC system could achieve an 83% fuel cell thermal capacity factor,

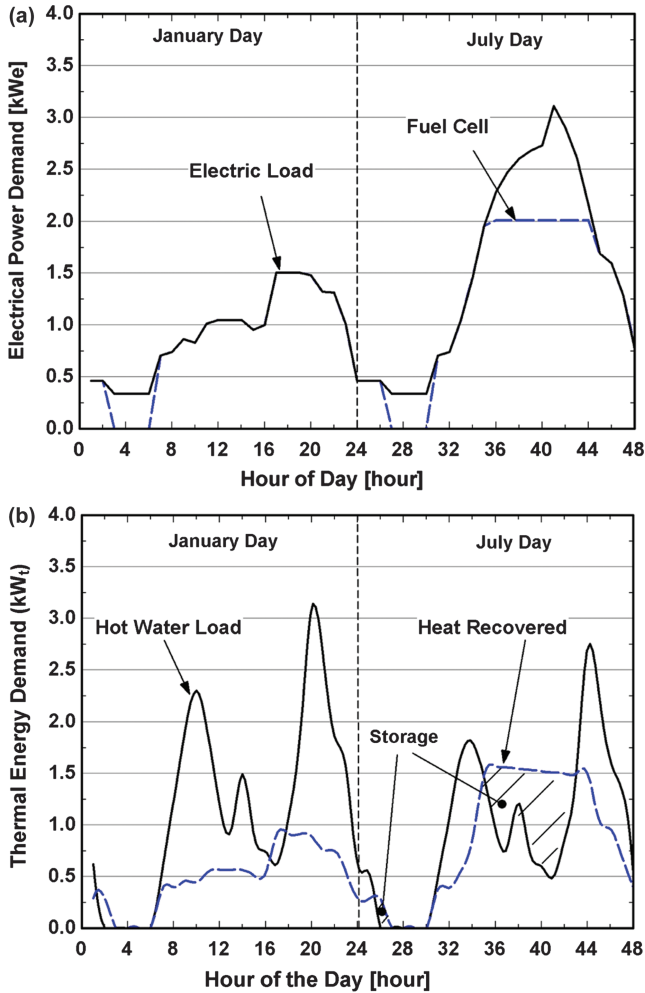


**Figure 12.13** (a) System load-following power output and building demand plot on two days of the year (b) system thermal energy output and building thermal demand plot on two days of the year.

displacing 6000 kWh of thermal energy that otherwise would have been served by a conventional hot water heater.

The 'home' capacity factors are indices that indicate the effectiveness of the fuel cell system in meeting the household electric or thermal loads. That is, it is the total kWh of electricity or thermal energy supplied by the fuel cell system divided by the total kWh household electricity or heat demanded. As system capacity is increased, the house electric capacity factor passes through a maximum at 2 kW and decreases with increasing system rating due to the system turndown limitations. From the viewpoint of meeting household electrical energy demand, a 2 kW system is energetically optimal. Thus, unless the

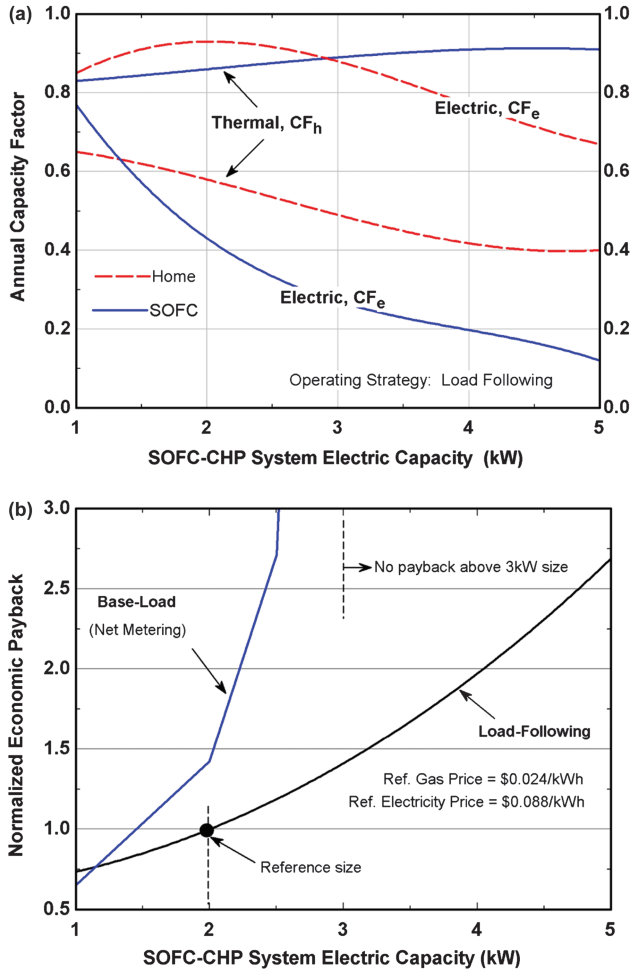


**Figure 12.14** (a) Influence of power rating on SOFC-CHP system and home capacity factors (b) influence of power rating and electric-led operating strategy on normalized payback economics.

system turndown capability can be substantially increased, a 5 kW SOFC system should not be employed in a load-following scenario for both economic and household energy effectiveness reasons.

Grid-connected SOFC systems benefit from buyback of electricity from the utility when excess power is produced. Utility electric purchase price agreements for renewable energy systems, such as solar photovoltaic systems, are at retail grid-electricity prices, however, that is not always the case for CHP systems. Surveys of net metering programmes in the U.S. indicate that the average utility will repurchase excess electricity at retail rates as long as there is no net electrical energy production onsite over the billing cycle (*i.e.*, running the meter backwards).<sup>85</sup> Once an SOFC-CHP system becomes a net power

producer, the utility will only buy back the power at avoided cost which typically ranges from 1.5 to 2.0 ¢/kWh.<sup>34</sup> Assuming a utility buy back rate of 2.0 ¢/kWh, Figure 12.14(b) provides a comparison of the economic effectiveness between electric-led load-following and base-load operating strategies as a function of SOFC system capacity where the payback is normalized to the 2-kW system payback period. In the base-load scenario, the SOFC system is operating in a net metering manner. As system size is increased, fewer savings are realized for the base-load scenario resulting in an infinite payback above 3 kW-sized fuel cell systems. A 1 kW-size SOFC system operating in a base-load configuration has the lowest economic payback period (*i.e.*, it is the most attractive) since it has high capacity factor and the lowest quantity of electrical energy purchased by the utility at the avoided cost. Figure 12.14(b) also shows that for single family residences, the economics grow less attractive with increasing system size as capital costs increase at a rate greater than the annual savings.

Annual simulations (8,760-hr) of a base-loaded 1-kW SOFC-CHP system produce an overall electric efficiency of 44.5%-LHV and a CHP efficiency of 84.6%-LHV. When operated in a load-following control strategy, the electric efficiency increases to 46.0%-LHV and the CHP efficiency to 85.5% due to more frequent part-load operation of the SOFC which results in higher efficiency. Despite the efficiency advantage of electric-led load-following operation, the base-loaded system produces a 10% lower payback period.

Since the SOFC system typically cannot respond to load changes very fast (slow dynamic response) without careful control and small energy storage, a thermal load tracking strategy can be attractive.<sup>49</sup> However, a thermally led, load-following strategy has some disadvantages. During the heating season the system produces too much electricity, which is only economic if it can be sold to the grid. Additionally, given the characteristically low TER of high-efficiency SOFC-CHP systems, sizing the system based on thermal demand requirements will result in a power capacity much higher than the application requires, thereby also resulting in much higher investment costs.

The amount of the heat recovered can strongly affect the overall economics of micro-CHP applications, but its value is also proportional to the price of natural gas. The lower the price of natural gas, the less influence the amount of waste heat recovered has on the value proposition. Moreover, a better indicator for the viability of CHP applications is the so-called 'spark spread,' which is defined as the price of grid electricity minus the price of pipeline natural gas. Plots of the normalized economic payback versus spark spread are given in Figure 12.15(a) for a 1 kW electrically-led, base-loaded SOFC system operating either as a CHP system or as a power-only system. The economic payback period of all plots is normalized against the SOFC-CHP ('cogen') system at the reference spark spread of 6.4 ¢/kWh. At this condition, the payback period is slightly over five years. There are several interesting features to note about the trends displayed in Figure 12.15(a). First, the analysis indicates that thermal energy recuperation yields a 60% lower economic payback at the reference spark spread and moreover, is more favourable than power-only systems

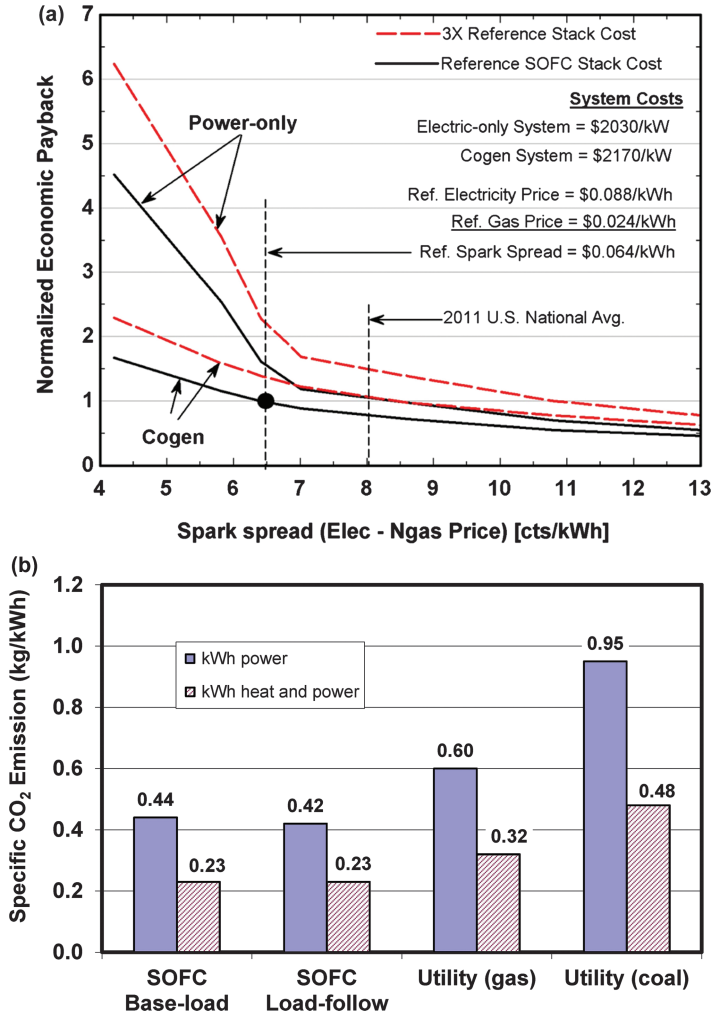


**Figure 12.15** (a) Economic sensitivity to utility pricing and SOFC capital cost (b) Comparative specific CO<sub>2</sub> emissions for base-loaded 1-kW SOFC system versus conventionally supplied energy.

irrespective of the spark spread for the range shown. As the price of either electricity or natural gas fluctuates, cogeneration to produce domestic hot water generally decreases the sensitivity of the economic outcome to utility pricing. Second, the value of thermal energy recuperated clearly increases with increasing natural gas price and in contrast, as electricity price increases, the economic importance of cogeneration is diminished. This result is supported by other studies which show that given the option to preferentially select between heat-led or electric-led load-following operation, electric-led is always chosen as the utility power buy-back rates approach the retail (*i.e.*, grid) residential rates.<sup>82</sup>

The preceding results are based on a mature SOFC stack cost of \$450/kW. Results are also presented for a stack cost three times this value to evaluate the economic sensitivity of early production units. The dashed lines in Figure 12.15(a) show that the payback period for both cogeneration and electric-only systems increases by about 40%, while yielding the same trends as the mature unit stack cost.

Figure 12.15(b) presents a comparison of the specific CO<sub>2</sub> emissions between a 1 kW SOFC system and the average U.S. utility<sup>86</sup> when supplying electrical and thermal energy (domestic hot water) to the residence. The base-load SOFC system achieves a CO<sub>2</sub> emission output at 0.44 kg/kWh-electric, and the load-following case is slightly lower at 0.42 kg/kWh-electric due to the slight efficiency advantage. Utility CO<sub>2</sub> emission rates are between 35 and 115% larger than the base-loaded fuel cell system output. The improved CO<sub>2</sub> emission characteristics in a CHP system result because the fuel utilized to provide power also supplies thermal energy to the residence.

The annual hourly average electric load of the single-family residential application in this example was about 1.0 kW. Sizing the SOFC system at 1 kW produced the lowest payback period, the highest fuel cell electric and thermal capacity factors, and the lowest annual CO<sub>2</sub> emissions. Further, operating in an electric-led, base-load control mode is more attractive both economically and technologically than load-following provided net metering plans are available. Lastly, cogeneration in the form of DHW supply to the household is preferable to power-only SOFC systems. The micro SOFC-CHP simulation results presented here suggest that for single-family detached dwellings, SOFC system size should be based on the annual hourly average electric demand of the application and that cogeneration is preferred over power-only systems.

It is important to note that these results are by no means conclusive as the study has not considered many other aspects and variables, such as heat-led operating strategies, different building loads and associated TERs for other home types, sizes, and geographic locations, and the influence of different policy measures (*e.g.*, carbon taxation, grid- and utility-related externalities, *etc.*) and regulations that could affect net metering plans and interconnection standards and fees. Nevertheless, the simulation proves to be illustrative of the considerations involved in residential micro-CHP applications.

## 12.5.2 Large-scale CHP and CCHP Applications

The application of SOFC-CHP systems in larger commercial and industrial applications is of interest to many developers and potential end-users. Renewable fuels such as landfill gas and biogas produced in anaerobic digesters from animal waste or in wastewater treatment plants present a unique opportunity for fuel cell CHP systems. Recent studies on the use of renewable biogas as a fuel feedstock for MW-class SOFC-CHP systems show that even though the fuel gas is typically diluted such that methane represents only 60% of the gas content, high electric efficiencies in the range of 45–52%-LHV and CHP efficiencies from 85–88%-LHV could be achieved.<sup>73,78</sup> The

potential life cycle costs of such systems have also been shown to be superior to large reciprocating IC engines, microturbines, molten carbonate fuel cell systems, and competitive with larger gas turbine technologies if SOFC technology can reach the mature costs that comes with high volume manufacturing.<sup>73</sup>

In large commercial building applications, the penetration of SOFC-CHP technology is challenged by many market barriers that are technology neutral (see Section 12.7). Yet recent work shows some promising options, particularly in SOFC-CHP operating strategies that favour *both* the end-user and the electric utility.<sup>2</sup> Business models that view the electric grid as a peaking plant are generally not attractive to electric utilities in the U.S. However, the SOFC as a dispatchable resource could be attractive to the utility if it was large enough so that it could serve the majority of the commercial building loads and export electric power to the grid during high peak demand time periods. Simulations of a 1.3 MW SOFC-CHP against experimentally measured energy demands for a large hotel indicate that CHP efficiencies over 85% can be achieved with less than 15% impact to the end-user COE.<sup>2</sup> Other work indicates additional promise for 1 MW SOFC-CHP systems serving residential neighbourhoods with electric power and district heating.<sup>88</sup>

The high-quality heat available in the exhaust gas of SOFC systems make them an attractive option for CCHP applications, especially in larger buildings (*e.g.* multifamily,<sup>45</sup> hospital, university,<sup>89</sup> governmental.)<sup>21</sup> The lower efficiency (and power) of conventional boiler and IC engine systems and the intermittent nature of solar power (especially the scarcity of solar radiation in winter time) make them less attractive in CCHP applications compared with SOFC systems. For example, a recent study comparing different renewable technologies for integration into a 500 kW CCHP building application found that an SOFC-based system has the highest electrical efficiency among these systems and can produce enough energy for supporting both the heating and cooling systems. In terms of maximum CCHP (*i.e.* trigeneration) efficiency, biomass- and solar-trigeneration systems are expected.<sup>44</sup> Integration of SOFCs with solar thermal collectors to form an integrated CCHP system for a university building located in Naples (Italy) with an electrical capacity of about 250 kW has also been explored. Simulation results indicate that the system can achieve a net electrical efficiency of nearly 47% and can overcome the severe issues regarding the thermal balance of PEM operating systems as well as the problems associated with the standalone solar systems.<sup>89</sup>

The potential advantages of SOFC-CCHP systems in term of both techno-economic and environmental issues for multifamily housing applications has been evaluated and compared with other competing technologies, such as the IC engine and natural gas boiler.<sup>45</sup> Using cell, stack and systems models,<sup>3,28,29</sup> a performance assessment of building-integrated SOFC-CCHP systems in different multifamily housing in the hot climate of Madrid (Spain) were assessed.<sup>45</sup> The system performances were determined in terms of

non-renewable primary energy demand and CO<sub>2</sub> equivalent (CO<sub>2</sub>-eq) emissions, and compared to a system with that employed an IC engine and with respect to the reference system. The reference system for all cases comprised a gas boiler and a mechanical chiller and grid-electricity supplied according to the selected generation mix. Compared to IC engine-based cogeneration and to traditional gas burner/mechanical chiller/grid electricity supply technology, significant savings in both energy (62%) and CO<sub>2</sub> emissions (35%) resulted from employing an SOFC trigeneration system, especially when an UCTE (union for the coordination of the transmission of electricity) electricity grid mix was assumed.<sup>45</sup>

Noteworthy studies are focusing on the technical assessment and optimization of such systems using different climates, building sizes and system configurations. For example, a CCHP system consisting of an SOFC system integrated with a double-effect water-lithium bromide (LiBr) absorption heating and cooling system was investigated<sup>21</sup> to assess its potential for supplying the space heating, cooling, hot water and lighting energy demands for an American office building of around 9500 m<sup>2</sup>.<sup>21</sup> Besides proofing the technical feasibility of such a system (total efficiency more than 87%), the study illustrated that the system can become economically competitive with CHP technologies when SOFC capital costs are reduced to about \$1000/kW and the life span of at least five years are reached.<sup>21</sup> The SOFC trigeneration system was predicted to achieve CCHP and CHP efficiencies about 89% and 84%, respectively which is higher than the typical values (70–80%) reported for similar systems using either IC engine or micro-gas turbines.

Presently, the authors are unaware of any hardware technology demonstrations of SOFC-CCHP systems in building applications. Nevertheless, the results of these case studies add to the growing body of technical literature that demonstrates technical feasibility and potentially superior performance of SOFC-based systems compared to both renewable and conventional technologies.

## **12.6 Commercial Developments of SOFC-CHP Systems**

During the last decade, demonstration projects on either small-scale or full-size systems have been started in various countries for verifying these characteristics under actual application conditions. The demonstration systems are largely focused on residential micro-CHP applications and although there are still various techno-economic issues, such as cost and complexity, the results show promise for the successful application of such systems in residential households. There is a growing number of successful pilot plants around the globe and several industrial companies have begun commercialization efforts of their SOFC products around the world.

The following sub-section synthesizes some of the commercialization efforts and demonstration projects related to SOFC-CHP systems. Based on the open

literature, the authors are unaware of any SOFC-CCHP system currently available on the market. The only practical fuel cell-CCHP system is developed by UTC Power<sup>90</sup> which integrates an absorption chiller with a phosphoric acid fuel cell to produce about 50 tons of cooling. As a result, SOFC-CHP systems development is the central focus in the following summary.

### 12.6.1 Commercialization Efforts

There are approximately six companies offering commercial (or 'pre-commercial') SOFC power system products. Ceramic Fuel Cells Limited Co. (CFCL) has about 20 years of experience in the development of SOFC stacks and offers SOFC-CHP units in the range between 1 and 5 kW.<sup>91,92</sup> CFCL offers two power modules (Gennex<sup>93</sup> and BlueGen<sup>94</sup>) that are intended to support different markets and customers. Gennex is a fuel cell power module fuelled by natural gas that has been designed for integration with existing appliances such as condensing boilers (which provide hot water and space heating) by sharing common inputs and outputs from the fuel cell.<sup>93</sup> BlueGen is a self-contained packaged system providing heat and power. The Gennex module comprises fuel cell stack, hot BoP (integrated steam generator, burner, and fuel & air heat exchanger), and high temperature insulation. The stack operates in the temperature range between 800 and 870 °C and is modular, starting with a base manufactured cell-stack containing 28 layers and producing about 150 W of DC power at 850 °C. Seven units form a 1 kW stack and 14 are needed for a 2 kW stack. Gennex documentation indicates that it can be power modulated from 0 to 2 kW with electrical efficiencies of around 57% at 2 kW (approximately 1000 W thermal output), 60% at 1.5 kW (approximately 540 W thermal output), and 36% at 0.5 kW (approximately 400 W thermal output).<sup>38,39</sup> The total thermal efficiency of the system is between 60 and 85 %, depending on the amount of heat recovered. The Gennex electrical and thermal efficiencies versus the exported power are shown in Figure 12.16 (based on exhaust gas cooled to 30 °C) and the unit has a reported start-up time of about 25 hours.<sup>93</sup>

The Bluegen unit<sup>94</sup> is a small-scale heat and power generator fuelled by natural gas that is approximately the size of a washing machine (600 mm×660 mm×1010 mm). The waste heat generated by the power module within BlueGen is used for production of hot water and is sufficient to provide 150–200 L of DHW per day. The system is optimized as an electrical generator with a peak electrical output of 2 kW at a maximum net AC electrical efficiency of 60%. The TER is less than 0.5 and the total thermal efficiency of the system can reach up to 85%, depending on the operating condition and amount of waste heat recovered. Specific CO<sub>2</sub> emissions are reported to be about 340 g/kWh.

Table 12.4 provides a summary of the commercial and demonstration SOFC systems including costs and demonstrated hours of operation.

Vaillant Group, has commercialized wall-hung heating appliances based on SOFC power systems. The system is designed for single-family houses and generates 2 kW of heat and 1 kW of electricity.<sup>95</sup> System development has been

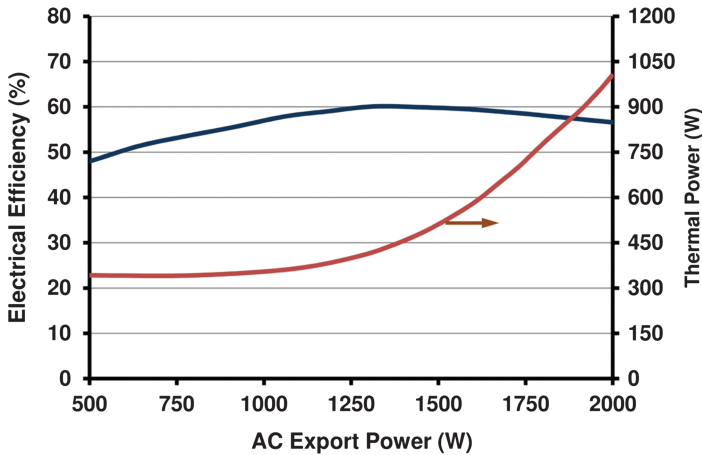


**Figure 12.16** Net electrical and thermal efficiencies of Gennex power module versus AC export power. (Adapted from Ref. 93.)

in cooperation with Staxera GmbH and the Fraunhofer Institute for Ceramic Technologies and Systems (IKTS) in Dresden.<sup>95</sup>

In the USA, Acumentrics has developed three SOFC systems (RP20, RP 1000/1500) suitable for micro-CHP applications. The company has reported installations at various sites in states such as Colorado, West Virginia, Texas, Arkansas, Pennsylvania, and in Calgary, Canada. The RP20 SOFC stack is built from tubular cells which operate near 800 °C. The net DC output of the stack is 1000 W. RP 1000/1500 are 2.5 kW (RP1500) and 2.0 kW (RP 1000) versions of RP series.<sup>96</sup>

Larger SOFC systems for commercial building applications have been commercialized by Bloom Energy. Two products are offered at either 100 or 200 kW capacities – the ES5400 and ES 5700, respectively. These units are power-only systems achieving net electric efficiencies greater than 50%-LHV.<sup>97</sup>

In Canada, DDI energy Inc. produces an SOFC-based power generator fuelled by natural gas, propane, and methane. System products range between 3 to 40 kW (ARC1-P3 to ARC2-P40) and are suitable for both indoor and outdoor installation.<sup>98</sup>

## 12.6.2 Demonstrations

SOFC technology demonstrations are numerous and varied with support and financial incentives provided by different governments and agencies. The following synthesizes some recent SOFC technology demonstration projects in Europe and Japan, as well as some companies, such as Topsoe Fuel Cells and Versa Power, who are leaders in SOFC technology but have not yet officially commercialized systems.

Hexis GmbH is focusing on stationary applications with an electric power output below 10 kW through their Galileo 1000N system. Systems have been

**Table 12.4** Summary of commercially available and demonstration SOFC systems intended for building applications.<sup>31,33,94,95,96,97,98,103,104,106</sup>

	Commercial products				Demonstration units			
	ARC Series (DDI Energy)	Bloom Energy (CFCL)	BlueGen (CFCL)	RP (AcumentricsCorp.)	ENE-FARM (Osaka Gas)	Vaillant EBZ	Galileo 1000N Hexis)	EnGen
Weight (kg)	273 to1180	19400	<200	136	94	-	170	17.5 (stack)
SOFC type	Planar	Planar	Planar	Tubular	FT-SIS	Planar	Circular	Planar
Fuel type	NG, Propane, Methane	NG	NG	NG, Propane	NG	NG	NG, LPG, biogas, Syngas	NG
Max. power (kW)	3 to 40	210	2	1, 2,2.5	0.7	1	1.5	0.5
AC electrical efficiency (LHV) (%)	-	>50	60 (at 1500 W)	>30	46.5	30	25-30	30 (Stack eff.)
Thermal output (W)	-	-	300 to 1000	-	470 W	2	2.5	-
Total efficiency (%)	60	-	85	-	90	85	>90	-
Flue gas Temperature (°C)	250-482	-	< 200	-	75	-	Condensate to ambient temp.	200-500
CO <sub>2</sub> (g/kWh)	578.70	350.6	340	-	690	-	.05	-
NO <sub>x</sub> (g/kWh)	0.037	<4.535	No	-	-	-	0.06	-
Cost (per kW) (US \$)	~47500 to 100,000	~8000	-	-	~33700 (0.7 kW system)	-	-	-

\* system developed by Tokyo Gas Co. has almost same characteristics.

\*\*Topsoe Fuel Cells and Versa Power, who are leaders in SOFC technology have not yet officially commercialized systems.

tested in houses and small apartment buildings for a reported duration of more than 27 000 hours (status as of October 2010) with a power degradation rate on power of approximately 2% per 1000 h.<sup>31</sup> These systems convert natural gas (or bio-methane) into electricity and heat using radial planar electrolyte-supported cells and metallic interconnects (60 repeat units).<sup>99</sup> The Galileo unit generates an electrical output of 1 kW and a thermal output of approximately 2 kW. Additional heat up to 20 kW can be generated by an integrated burner. The system electrical and overall efficiencies are 30–35% and >90%-LHV, respectively, with low emissions of NO<sub>x</sub> (<30 mg/kWh) and CO (<30 mg/kWh).<sup>99,100</sup>

EBZ is developing planar SOFC stacks and systems (with a focus on stationary heating appliances and small CHP). Development efforts have been in conjunction with the FP7 EU-collaborative project FC-DISTRICT. Participants of this project come from 23 European organizations and companies. One of the main objectives of the FC-DISTRICT project is to develop SOFC-CHP systems which are able to produce up to 2 kW electric power and 6–8 kW thermal power with an overall efficiency up to 90%-LHV.<sup>33</sup> In the framework of this project, as well as the Flame SOFC project, EBZ's SOFC micro-CHP units have been designed to generate a nominal power output of 1.5 kW electric and 2.75 kW thermal at 30% net electrical efficiency. The targeted overall efficiency of this system is above 90%. The EBZ system operates with several fuels such as natural gas and biogas and employs catalytic partial oxidation to convert the fuel to a hydrogen-rich fuel gas. System emissions are reported to be NO<sub>x</sub> < 60 mg/kWh, CO < 50 mg/kWh at 0% O<sub>2</sub>.<sup>101,102</sup> The electrolyte-supported SOFC stack used in this system is developed by Staxera GmbH.<sup>33</sup>

The EnGen unit is a complete SOFC micro-CHP demonstration system with net power production up to 1000 W. The system is developed through collaboration between Htceramix (Switzerland) and SOFCpower (Italy). The system operates on natural gas that is reformed through a catalytic partial oxidation (CPOx) reactor and achieves electric efficiencies in the range of 30–32%.<sup>103</sup> The complete system is fully autonomous with a lead-acid battery for grid-independent start-up, UPS functionality, and for surge coverage. The packaged system includes heat exchanger, temperature insulation, electric heater for start-up, smart temperature control, voltage conditioning for a lead acid battery compatible output and integrated software and controls.<sup>103</sup>

Since 2004, the Japanese companies, Tokyo Gas, Rinnai, and Kyocera (stack manufacturer) jointly with Gstar Exploration Ltd. (USA) are focusing on CHP systems development based on flatten tubular segmented-in-series (FT-SIS) SOFCs.<sup>104,105</sup> This specific cell design can reduce the gas sealing problem (same as tubular design) and has also more stable electrical connections (same as segmented-in-series cells). The cell has also high durability at high temperature since it is completely made of ceramic materials.<sup>32</sup> The first residential CHP system using the above technology was developed in 2008 and has been implemented into several homes for data collection under realistic conditions. Each stack is composed of two bundles of 36 FT-SIS cells

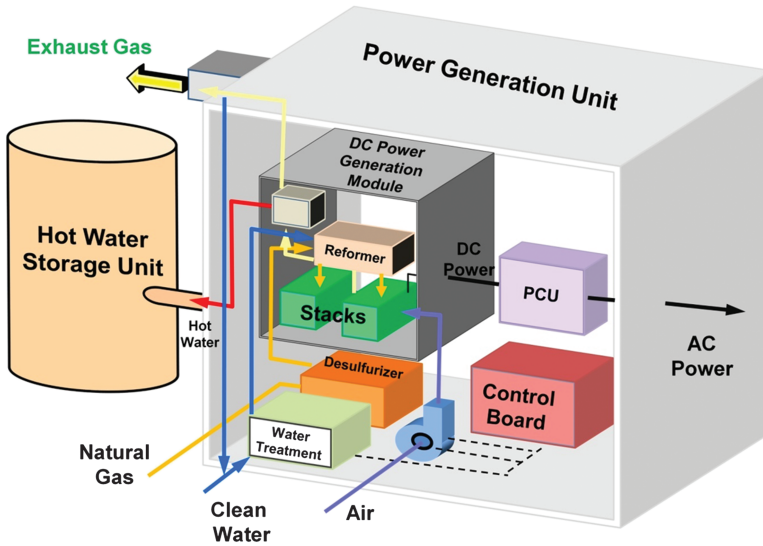


**Figure 12.17** Schematic of Packaged FT-SIS SOFC system developed by several Japanese companies. (Adapted from Ref. 104.)

each and can generate almost 800 W (11 W each single cell). The electrical and heating efficiencies of this system are more than 40% and 32% at 700 W respectively. A conceptual overview of the packaged system is shown in Figure 12.17.

The ENE-FARM Type S is a SOF-CHP system developed with collaboration work between Kyocera, Osaka Gas, Aisin Seiki, Chofu Seisakusho, and Toyota Motor Corporation. This system involves the same stack as mentioned above (from Kyocera). This 700 W system costs about (¥2.75 million (US \$33,700) (including taxes but excluding) costs.<sup>106</sup>

In Finland, the technical research centre of Finland (VTT) and Wärtsilä have been jointly working on developing of SOFC-CHP systems for both residential and industrial applications, but hardware demonstrations have been for systems in the range of 5–10 kW<sub>e</sub>. VTT has also a strong participation in several European programs such as Large SOFC and SOFC600. The VTT SOFC system is designed to work with natural gas using a planar anode-supported stack (counter-flow design with internal manifold) obtained from Forschungszentrum – Jülich. The stack comprises 50 rectangular unit cells with an active area of 361 cm<sup>2</sup>. Ambient air is supplied to the system with two blowers (3–10 air excess ratio). The maximum DC power ( $P_{el,stack}$ ) and DC efficiency ( $\eta_{el,stack}$ ), are about 5 kW and 50% (LHV) respectively.<sup>107</sup> In 2009, VTT developed a 10 kW demonstration unit jointly with Versa Power Systems.<sup>108</sup>

Topsoe Fuel Cell (TOFC) focuses on the technical development and commercialization of SOFCs. The POWERCORE module has been developed for CHP applications with system integration in collaboration with Dantherm Power.<sup>109,110</sup> The TOFC POWERCORE is developed for single-family

households with an average power demand of 1 kW nominal electrical power. The system operates with natural gas but additional fuels, such as methanol, LPG and biofuels are also expected in the future.<sup>7</sup> The system is comprised of several components such as insulation, start-up burner, heat exchanger, reformer, stack, off-gas burner and instrumentation. The DC efficiency and fuel utilization of the PowerCore unit are in the power range 750–1350W at about 60–65% and 80–85%, respectively.<sup>7</sup>

The potential market for small SOFC systems has also encouraged other U.S. SOFC developers and laboratories to produce demonstration units. As noted previously, Versa Power Systems jointly with VTT (Finland) is developing a 10 kW system for commercial building applications. Recently, Pacific Northwest National Laboratory (PNNL) reported the installation of a high efficiency 2 kW SOFC power-only system.<sup>111</sup> This system consists of four parallel planar anode-supported stacks provided by Delphi Corporation, one steam reformer, five recuperators (four in the cathode side and one in the anode loop), one condenser, and two blowers (in both anode and cathode loops). Each stack involves 30 cells, each with an active area of 105 cm<sup>2</sup>. The system was designed so that about 83–90% of anode exhaust stream can be recycled. The reported electric efficiency record for this system is about 57%-LHV which is significantly higher than the performance reported elsewhere for similarly sized systems (*i.e.*, 30–50%-LHV).<sup>21</sup>

## 12.7 Market Barriers and Challenges

The widespread deployment of SOFC-based CHP and CCHP systems in DG applications provides an attractive alternative as a global energy solution to the 21<sup>st</sup>-century problems of energy shortages, security, and access to low-cost energy supplies, grid congestion, reliability, and power quality, and reduction of harmful energy-related emissions. In general, many experts observe that the increase in CHP/CCHP system deployment (inclusive of gas and steam turbines and IC engines) is a growing trend in energy supply around the world and that the potential benefits are manifold.<sup>19,22,112</sup> For example, over the last 15 years, Japan has increased its CCHP installations from less than 1 MW to over 10 GW; the U.S. has now over 85 GW of installed CHP/CCHP; and China has announced the goal of over 40 GW of new CCHP installations by 2020.<sup>113</sup> In contrast to conventional CCHP system technologies, such as gas turbines and IC engines, an SOFC-based energy technology platform is unique in its ability to serve as a scalable, fuel flexible, highly efficient, low-emission, and potentially cost-effective polygenerator of cooling, heat, fuel and power. In the following sub-sections, we discuss the outlook for application of SOFC-CHP/CCHP systems in CHP markets from the viewpoints of energy prices, capital and life cycle costs, and regulatory policy and environmental impact.

### 12.7.1 Energy Pricing

The long-term viability of SOFC technology is closely related to being able to provide a market solution with low life cycle costs (*i.e.*, low capital and operating

costs). As previously discussed in Section 12.5, the spark spread strongly influences the life cycle costs of an SOFC-CHP/CCHP system. The larger the spark spread, the more economically attractive onsite CHP installations become. The shale gas revolution in the United States has lowered natural gas prices to their lowest levels in over a decade such that average city-gate natural gas prices ( $\sim 4.55$  \$/GJ in 2011) are now cheaper than coal per unit of energy.<sup>114</sup> Furthermore, the substantial increase in unconventional natural gas resources (over 35% of U.S. gas production in 2011) has dramatically improved gas supply stability such that natural gas prices have become independent and decoupled from petroleum prices while retail U.S. electricity prices have been relatively flat for the last five years.<sup>114,115</sup> The supply of cheap natural gas has created a substantial shift away from coal-based power generation from over 50% of the U.S. generation mix to less than 37% in just ten years time. Renewable biogas fuels derived from landfill and anaerobic digester gas resources also offer attractively low fuel prices. In the short-term, historically high spark spreads are promoting increased interest in CHP in general.<sup>112</sup> Because of the relationship between natural gas and electricity prices, it is now believed that over the long term (*i.e.*,  $\sim 20$ -years), the forecasted increase in U.S. natural gas supply combined with reduced electricity demand (*e.g.*, due to increased 'green' building infrastructure and energy conservation efforts in the commercial building sector) will lead to substantially reduced retail electricity prices which may gradually reduce current spark-spreads in some countries.<sup>116,117</sup>

### 12.7.2 SOFC Costs

Capital cost reduction of SOFC stacks have made remarkable progress over the last ten years, dropping by nearly an order of magnitude to about \$175/kW in high volume production scenarios.<sup>118</sup> At the system-level, capital costs of mass-produced 1–2 kW SOFC-CHP systems have been estimated at about 2300 US\$/kW which is shown to compete with conventionally supplied grid-electricity and natural gas fired boilers when the systems are optimally designed.<sup>41</sup> These systems are marginally competitive without incentives when U.S. averaged utility energy pricing for electricity and natural gas are employed. Capital costs for larger-scale SOFC-CHP systems are expected to range from 1950 US\$/kW to 1120 US\$/kW for systems sized at 330 kW and 6.0 MW, respectively.<sup>73</sup> These capital cost estimates are consistent with other recent larger-scale SOFC-CHP manufacturing cost studies.<sup>119</sup> The resulting cost of electricity for such larger systems is estimated to range from 0.079 to 0.050 US\$/kWh, which is lower than commercial grid-electricity prices, and on par with industrial electricity prices in the U.S. These business-as-usual value propositions show that even mature SOFC technology in mass production scenarios, while competitive in some market sectors, are not as compelling and representative as they could be given the environmental, societal and energy reliability and security benefits associated with widespread implementation of distributed generation.

### 12.7.3 Technical Barriers

Interest in SOFCs for mobile APU, UAV, and UUV applications<sup>120–122</sup> and residential micro-CHP<sup>33,39,47,48</sup> has increased dramatically within the last 10 years and is partly driven by the congruency of current SOFC system capacities (1–25 kW) with the application power requirements. While the residential sector has substantial room for improvements in energy efficiency, it is also one of the most challenging markets to compete in. Despite the efficiency advantages of high temperature fuel cell systems for onsite CHP generation, the application requirements of low maintenance, high durability or lifetime, low cost, and high efficiency are severe. Section 12.6 of this chapter has already discussed current manufacturers and operational systems. However, it should be noted that SOFC-CHP systems are not strictly limited to stationary applications. There is also interest in mobile SOFC-CHP systems. In particular exploratory studies of have illustrated the potential economic benefits and system architectures if metal-supported SOFC technology at 300–400 kW scales is employed as a gas turbine APU replacement in commercial aircraft applications.<sup>121</sup>

Technical issues for SOFC commercialization include cost reduction, durability improvement, and dynamic operation. In general, while technical issues related to SOFC capital cost and durability are often cited as barriers to widespread adoption of the technology, system integration and viable business models in all applications remains as a key scientific challenge, particularly for CCHP systems. System integration challenges encompass establishing: (1) the optimal system architectures for effective utilization of the different grades of thermal energy for export to the building application, (2) viable operating and control strategies (*e.g.*, heat-led *vs.* power-led; load-following *vs.* base-load, *etc.*) that are mutually attractive to end-user, electric utilities, and the SOFC technology itself, (3) power conditioning topologies and the associated technology to enable power plant islanding modes when grid-connected, and (4) the various forms of energy and resources that can be integrated to maximize benefits of fuel cell systems for both electrical energy generation, thermal energy utilization, and low environmental impact.<sup>17,23,123</sup>

### 12.7.4 Market Barriers and Environmental Impact

The economic picture is increasingly favourable towards SOFC-CHP system deployment in stationary applications; yet excitement surrounding the technology is tempered by the reality of persistent market barriers in many countries to all DG technologies. Indeed, while numerous organizations and countries throughout the globe have initiated meaningful product development efforts of (mostly small-scale) SOFC-CHP systems, complex commercialization barriers remain before widespread market penetration is realized. These barriers are technology neutral and are comprised of both technological and regulatory components that include, but are not limited to:<sup>17,22</sup>

- high first cost for turn-key installation,
- a ‘wait-and-see’ approach regarding adopting an onsite CHP energy supply system,

- regulated fees and tariffs associated with grid-electricity rate structures,
- unfavourable and non-standardized governmental policies and regulations,
- utility interconnection barriers and predatory pricing,
- low electricity buy-back rates from electric utilities,
- historic natural gas price volatility and customer resistance to power purchase agreements and
- limited liberalization of electricity markets worldwide.

While many of the barriers to DG installations are technology neutral and are common throughout the world, there are regional differences. In North America, excessive utility standby and backup power charges during CHP system downtimes detrimentally affect the attractiveness of CHP, as well as difficulties in securing long-term power purchase agreements from potential customers.<sup>112</sup> In contrast, many utility companies in Europe are not competing for customers and therefore, are often partners for DG implementation as they believe the CHP/CCHP investor is alleviating the utility of some capital risk associated with transmission and distribution (T&D) and generating capacity expansion.<sup>112</sup> However, in Germany, liberalization of the electricity market initially resulted in price wars which drove the grid electricity price below production costs before government policies favouring CHP were adopted.<sup>19</sup> The relatively high cost of natural gas in China means that nearly 95% of CCHP is fuelled by coal and is generally 10 to 100 MW in capacity, which limits energy conversion systems to conventional boilers and steam turbines as coal does not suit small- and intermediate-scale SOFC technology. However, fuel diversification is receiving increased attention in China with growing interest in biomass and biogas resources.<sup>19</sup>

Even though cost reduction and durability performance have dramatically improved, a primary challenge for SOFC technology in stationary CHP/CCHP applications is the lack of policy incentives that will enable all (or even some) of the associated externalities and societal benefits from technology adoption to be internalized such that the resulting value proposition is a compelling one. Recent studies indicate that if even modest sustainability policy measures are adopted, a viable market for mass production of SOFC-CHP systems would be established in the medium- to long-term (*i.e.*, within 20 to 30 years), which would enable expected cost targets to be achieved.<sup>75,117,124</sup> Aggressive policy incentives for fuel cell CHP systems adoption are predicted to create a large and sustainable market in European countries such as Germany.<sup>117</sup> In the U.S., a government-led objective of adding 40 GW of new, cost-effective CHP by 2020 has been announced with initiation of corresponding efforts at reducing market barriers.<sup>125</sup> If successful, this initiative could help catalyze widespread adoption of CHP/CCHP technologies for distributed generation with positive effects for the SOFC industry.

While environmental impact awareness and health concerns are increasing internationally, challenges to internalizing the environmental and societal benefits of highly efficient and environmentally preferred advanced energy

conversion systems, such as SOFC-CCHP technologies, remain. Traditional utility, industrial and commercial sector benefit-cost analyses include only transparent, market-traded monetary values; and thus, externalities, which may be significant, are largely ignored due to difficulties in value quantification.<sup>126</sup> The substantial benefits in terms of environmental impact of SOFC-based power generation systems for CHP applications have been evaluated through life cycle assessment studies which show that small- and large-scale SOFC technology is superior to both conventional competing technologies and the expected future utility electricity generation mix in almost all impact categories.<sup>127–129</sup> For example, one study found that the SOFC produces 70% less acidification than a low-NO<sub>x</sub> gas turbine and 30% less than a modern natural gas combined cycle plant on a life-cycle basis.<sup>128</sup> Cradle-to-grave (*i.e.*, product life cycle) energy and carbon payback times for micro SOFC-CHP systems have been estimated to range from 0.5 to 1.5 years and are even lower than renewable solar PV and micro-wind installations despite the conservative SOFC efficiency performance employed in the study.<sup>129</sup>

Efforts have also recently been made to quantify the benefits of fuel cell-based CHP/CCHP installations in term of the cost of electricity by assessing the value of generation-related, grid-related, and emissions- and health-related benefits.<sup>130,131</sup> When the benefits of fuel cell-based CHP/CCHP systems in the three aforementioned categories are rationally monetized, the resulting value, expressed in terms of cost of electricity, is estimated to range from 0.051–0.199 US\$/kWh.<sup>126</sup> A breakdown of category contributions is shown in Figure 12.18, illustrating that health benefits, avoidance of grid-related costs, and avoidance of generation-related costs can amount to 8.49, 2.34, and 9.12 US\$/kWh, respectively. Further, by employing waste heat recovery for CHP/CCHP purposes, the value proposition is increased by over 50% compared with power-only systems.<sup>131</sup>

Alternatively, another perspective when evaluating the merit of fuel cell-based CHP systems is to analyze the externalities of existing conventional

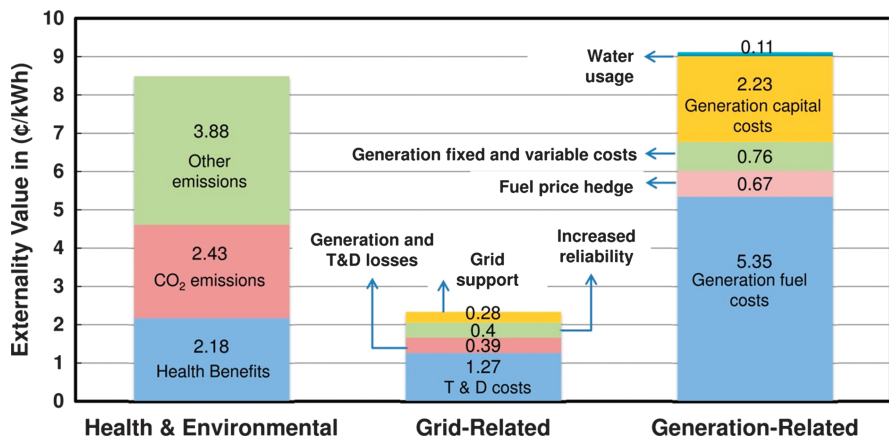


**Figure 12.18** Valuation of externality benefits associated with fuel cell-CHP/CCHP systems in terms cost of electricity.

power generation and consider pricing them into the price of electricity. Coal-based power generation in the U.S. has historically accounted for over 50% of the electricity generation mix (it is less than 38% as of 2012). Moreover, at least one recent study estimates that when the costs external to the coal industry (*i.e.*, environmental and health damages associated with coal extraction, transport, processing, and combustion) are accounted for, the effective price of electricity per kWh of generation is conservatively doubled to tripled in the U.S., thereby making renewable and alternative forms of power generation ‘economically competitive’.<sup>132</sup> Thus, either of these analysis viewpoints makes a compelling case for the deployment of SOFC-CHP/CCHP systems when the externalities associated with environmental and health effects are rationally valued and reflected in the price of energy supplies.

## 12.8 Summary

The unique and beneficial characteristics of SOFC technology, coupled with emerging energy production and supply paradigms related to distributed generation, hold much promise for their eventual widespread adoption in numerous residential and commercial building applications. A study of building energy demand characteristics and results from numerous SOFC system simulations indicate that the high efficiency and low thermal-to-electric ratio characteristics of SOFC-CHP systems can provide greater energetic, economic and environmental benefits than competing technologies, including renewables and other fuel cell types. Black and grey box system modelling approaches (including techno-economic modelling) are typically employed in SOFC-CHP/CCHP system performance estimations and application simulations. Performance expectations gathered from numerous studies as well as an examination of the current commercial offerings in SOFC-CHP and power-only systems indicate system electric efficiencies greater than 50%-LHV and CHP efficiencies greater than 85%-LHV are readily achievable. Hardware-based SOFC systems incorporating thermally activated cooling technologies to form an integrated SOFC-CCHP system have not yet been realized, but are of increasing interest globally as distributed polygeneration presents compelling solutions for emerging energy supply, reliability, and efficiency challenges. SOFC technology is not yet mature, and faces cost reduction, durability improvement, and robust dynamic operation challenges before widespread adoption in competitive building energy sectors can take place. Additionally, market barriers applicable to all DG technologies are numerous and varied and represent a potentially much greater challenge than technical barriers for substantial penetration of new CHP/CCHP technologies.

## References

1. A. Verma and A. D. Rao, *J. Power Sources*, 2006, **158**, 417.
2. K. Nanaeda, F. Mueller and J. Brouwer, *J. Power Sources*, 2010, **195**, 3176.

3. E. Liese and J. Eng, *Gas Turbines Power*, 2010, **132**, 061703.
4. R. J. Braun, S. Kameswaran, J. Yamanis and E. Sun, *J. Eng. Gas Turbines Power*, 2012, **134**, 021801–1.
5. T. Tang, M. Pastula and B. Borglu, *ECS Trans.*, 2011, **35**, 63.
6. F. Mitlitsky, *Low-cost Co-production of Hydrogen and Electricity*, DOE Annual Merit Review Proceedings, 2008, [http://www.hydrogen.energy.gov/annual\\_review08\\_fuelcells.html](http://www.hydrogen.energy.gov/annual_review08_fuelcells.html).
7. H. Holm-Larsen, M. J. Jørgensen, N. Christiansen, J. H. Jacobsen, Paper presented at Fuel Cell Seminar, Uncasville, CT, 2012.
8. A. Nanjou, Proceedings of the 10th European SOFC Forum, Lucerne, Switzerland, 2012.
9. K. Föger Proceedings of the 10th European SOFC Forum, Lucerne, Switzerland, 2012.
10. Quadrennial Technology Review Framing Document, U.S. DOE, Washington D.C., 2011, [http://energy.gov/sites/prod/files/edg/qtr/documents/DOE-QTR\\_Framing.pdf](http://energy.gov/sites/prod/files/edg/qtr/documents/DOE-QTR_Framing.pdf).
11. R. Lasseter, A. Akhil, C. Marnay, J. Stephens, J. Dagle, R. Guttromson, A. S. Meliopoulos, R. Yinger, J. Eto, Integration of Distributed Energy Resources: The CERTS MicroGrid Concept, U.S. DOE, Washington D.C., LBNL-50829, 2002.
12. J. M. Guerrero, F. Blaabjerg and T. Zhelev, *IEEE Ind. Electron. Mag.*, 2010.
13. K. Hemmes, J. M. Guerrero and T. Zhelev, *Chem. Eng. Process*, 2012, **51**, 18.
14. C. Wendel, R. J. Braun, Proceedings of the 10th European SOFC Forum, Lucerne, Switzerland, 2012.
15. D. M. Bierschenk, J. R. Wilson and S. A. Barnett, *Energy Environ. Sci.*, 2011, **4**, 944.
16. W. L. Becker, R. J. Braun, M. Penev and M. Melaina, *Energy*, 2012, **47**, 99.
17. J. A. P. Lopes, N. Hatzigiorgiariou, J. Mutale, P. Djapic and N. Jenkins, *Electr. Power Syst. Res.*, 2007, **77**, 1189.
18. G. Chicco and P. Mancarella, *Renewable Sustainable Energy Rev.*, 2009, **13**, 535.
19. D. W. Wu and R. Z. Wang, *Prog. Energy Combust. Sci.*, 2006, **32**, 459.
20. J. Wang, Z. Zhai, Y. Jing, X. Zhang and C. Zhang, *Appl. Energy*, 2011, **88**, 5143.
21. F. Zink, Y. Lu and L. Schaefer, *Energy Convers. Manage.*, 2007, **48**, 809.
22. A. Shipley, A. Hampson, B. Hedman, P. Garland, P. Bautista, *Combined Heat and Power: Effective Energy Solutions for a Sustainable Future*, Oak Ridge National Laboratory, TN, 2008
23. R. J. Braun, S. A. Klein and D.T. Reindl, *J. Power Sources.*, 2006, **158**, 1290.
24. EnergyPlus Energy Simulation Software, <http://apps1.eere.energy.gov/buildings/energyplus/>.
25. P. Torcellini, M. Deru, B. Griffith, K. Benne, *DOE Commercial Building Benchmark Models*, National Renewable Energy Laboratory, Golden, CO, 2008.

26. R. J. Braun, S. A. Klein and D. T. Reindl, *ASHRAE Trans.*, 2004, **110**, part I.
27. *TRNSYS- A TRAnSient SYstems Simulation Program*, <http://sel.me.wisc.edu/trnsys/faq/faq.htm>.
28. P. Kazempoor, F. Ommi and F. V. Dorer, *J. Power Sources*, 2011, **196**, 8948.
29. P. Kazempoor, F. Dorer and F. Ommi, *Fuel Cells*, 2010, **10**, 1074.
30. CFCL BlueGen units for Virtual Power Plant Project in Netherlands. *Fuel Cells Bulletin*, 2012, **7**, 3.
31. A. Mai, B. Iwanschitz, U. Weissen, R. Denzler, D. Haberstock, V. Nerlich and A. Schuler, *ECS Trans.*, 2011, **35**, 87.
32. H. Yoshida, T. Seyama, T. Sobue and S. Yamashita, *ECS Trans.*, 2011, 97.
33. I. Frenzel, A. Loukou, D. Trimis, F. Schroeter, L. Mir, R. Marin, B. Egilegor, J. Manzanedo, G. Raju, M. D. Bruijne, R. Wesseling, S. Fernandes, J. M. C. Pereira, G. Vourliotakis, M. Founti and O. Posdziech, *Energy Procedia*, 2012, **28**, 170.
34. R. J. Braun, *Optimal Design and Operation of Solid Oxide Fuel Cell Systems for Small-Scale Stationary Applications*, PhD Thesis, University of Wisconsin-Madison, 2002.
35. S. H. Pyke, A. J. Burnett, R. T. Leah. *System Development for Planar SOFC Based Power Plant*, Harwell Laboratory, Energy Technology Support Unit, 2002.
36. I. Beausoleil-Morrison, *Annex 42 Final Report*, International Energy Agency, Canada, 2008.
37. P. J. Mago and A. K. Hueffe, *Energy and Buildings*, 2010, **42**, 1628.
38. R. J. Kee, H. Zhu, R. J. Braun, T. L. Vincent, *Advances in Chemical Engineering, Fuel Cell Engineering* K. Sundmacher, Elsevier, New York, NY, 2012, 41, 6, 331.
39. P. Kazempoor, V. Dorer and F. Ommi, *Int. J. Hydrogen Energy*, 2009, **34**, 8630.
40. K. J. Kattke and R. J. Braun, *J. Fuel Cell Sci. Technol.*, 2011, **8**, 021009.
41. R. J. Braun, *J. Fuel Cell Sci. Technol.*, 2010, **7**, 031018.
42. D. Bohn, Micro Gas Turbines. Rhode-St-Genèse, Belgium, RTO/NATO, 2005.
43. Z. Yu, J. Han and X. Cao, *Int. J. Hydrogen Energy*, 2011, **36**, 1256.
44. F. A. Al-Sulaiman and I. Dincer, *Int. J. Hydrogen Energy*, 2010, **35**, 5104.
45. P. Kazempoor, V. Dorer and A. Weber., *Int. J. Hydrogen Energy*, 2011, **36**, 13241.
46. W. L. Becker, R. J. Braun, M. Penev and M. Melaina, *J. Power Sources*, 2012, **34**, 200.
47. S. Farhad, F. Hamdullahpur, Y. Yoo, *Int. J. Hydrogen Energy*, 2010, **35**, 3758.
48. V. Dorer and A. Weber, *Energy Convers. Manage.*, 2009, **50**, 648.
49. V. Dorer, R. Weber and A. Weber, *Energy and Buildings*, 2005, **37**, 1132.
50. K. H. Lee and R. K. Strand, *Renewable Energy*, 2009, **34**, 2839.

51. ESP-r, an integrated building/plant simulation tool, <http://www.esru.strath.ac.uk/Programs/ESP-r.htm>.
52. BEopt-Building Energy Optimization software, <http://beopt.nrel.gov/home>.
53. N. Kelly, I. Beausoleil-Morrison, *Annex 42 Final Report: A Report of Subtask B*, International Energy Agency, Canada, 2007.
54. Aspen Plus - AspenTech, [www.aspentech.com/products/aspen-plus.aspx](http://www.aspentech.com/products/aspen-plus.aspx).
55. gPROMS -Process Systems Enterprise, <http://www.psenterprise.com/gproms>.
56. Engineering Equation Solver (EES). F-Chart Software. 2000. [www.fchart.com](http://www.fchart.com).
57. M. Burer, K. Tanaka, D. Favrat and K. Yamada, *Energy*, 2003, **28**, 497.
58. S. H. Chan, K. A. Khor and Z. T. Xia, *J. Power Sources*, 2001, **93**, 130.
59. H. Zhu and R. J. Kee., *J. Power Sources*, 2003, **117**, 61.
60. R. Bove, P. Lunghi and N. M. Sammes, *Int. J. Hydrogen Energy*, 2005, **30**, 181.
61. R. J. Braun, T. L. Vincent, H. Zhu, R. J. Kee, *Advances in Chemical Engineering: Fuel Cell Engineering*, ed. K. Sundmacher, Elsevier, New York, NY, 2012, 41, 7, 383.
62. E. Achenbach, U. Reus, 6th International Symposium on Solid Oxide Fuel Cells (SOFC-VI), Honolulu, Hawaii, 1999.
63. S. C. Singhal, K. Kendal, *High Temperature and Solid Oxide Fuel Cells, Fundamentals, Design and Applications*, Oxford, UK, Elsevier, 2003.
64. K. J. Kattke, R. J. Braun, A. M. Colclasure and G. Goldin, *J. Power Sources*, 2011, **196**, 3790.
65. F. Zhao and A. V. Virkar, *J. Power Sources*, 2005, **141**, 79.
66. S. Koch, Contact Resistance of Ceramic Interfaces Between Materials Used for Solid Oxide Fuel Cell, PhD Thesis, Risø National Laboratory, Denmark, 2002.
67. J. E. O'Brien, C. M. Stoots and J. S. Herring, *J. Fuel Cell Sci. Technol.*, 2006, **3**, 213.
68. D. H. Jeon, J. H. Nam and C. J. Kim, *J. Electrochem. Soc.*, 2006, **153**, A406.
69. S. Liu, C. Song and Z. Lin, *J. Power Sources*, 2008, **183**, 214.
70. C. M. Stoots, J. E. O'Brien, J. J. Hartvigsen. *Test Results of High Temperature Steam/CO<sub>2</sub> Co-Electrolysis in a 10-Cell Stack*, Idaho National Laboratory, 2007, [www.inl.gov/technicalpublications/documents/3751099.pdf](http://www.inl.gov/technicalpublications/documents/3751099.pdf).
71. R. J. Boersma and N. M. Sammes, *J. Power Sources*, 1996, **63**, 215.
72. R. J. Kee, P. Korada, K. Walters and M. Pavol, *J. Power Sources*, 2002, **109**, 148.
73. A. Trendewicz, R. J. Braun, *J. Power Sources*, 2013, **233**, 380.
74. K. Gerdes, E. Grol, D. Keairns, R. Newby, *Integrated Gasification Fuel Cell Performance and Cost Assessment*, U.S. DOE, DOE/NETL-2009/1361, 2009.
75. J. H. J. S. Thijssen, *The Impact of Scale-up and Production Volume on SOFC Manufacturing Cost*, Final report prepared for the U.S. DOE, 2007.

76. N. Autissier, F. Palazi, F. Maréchal, J. N. Herle and D. Favrat, *J. Fuel Cell Sci. Technol.*, 2007, **4**, 123.
77. F. Palazzi, N. Autissier, F. Marechal and D. Favrat, *Appl. Therm. Eng.*, 2007, **27**, 2703.
78. K. A. Pruitt, R. J. Braun and A. M. Newman, *Appl. Energy*, 2013, **102**, 386.
79. Table A2. Energy Consumption by Sector and Source, Annual Energy Outlook, Washington D.C., Energy Information Administration, U.S. DOE, Washington D.C., 2009, [http://www.eia.gov/oiaf/aeo/pdf/0383\(2009\).pdf](http://www.eia.gov/oiaf/aeo/pdf/0383(2009).pdf).
80. Table CE3.1 Household site End-use Consumption in the U.S, Totals and Averages, Residential Energy Consumption Survey, Energy Information Administration, U.S. DOE, Washington D.C., 2009, [http://www.eia.gov/oiaf/aeo/pdf/0383\(2009\).pdf](http://www.eia.gov/oiaf/aeo/pdf/0383(2009).pdf).
81. A. D. Hawkes, P. Aguiar, B. Croxford, M. A. Leach, C. S. Adjiman and N. P. Brandon, *J. Power Sources*, 2007, **164**, 260.
82. A. D. Hawkes and M. A. Leach, *Energy*, 2007, **32**, 711.
83. T. DeValve, B. Olsommer, *Micro-CHP Systems for Residential Applications Final Report*, Prepared by United Technologies Research Center for U.S. DOE, <http://www.osti.gov/bridge/servlets/purl/921640-8RSmr0/921640.pdf>.
84. A. D. Hawkes, P. Aguiar, C. A. Hernandez-Aramburo, M. A. Leach, N. P. Brandon, T. C. Green and C. S. Adjiman, *Energy Environ. Sci.*, 2009, **2**, 729.
85. Network for New Energy Choices in Freeing the Grid, New York, 2010. [http://www.gracelinks.org/media/pdf/freeing\\_the\\_grid\\_2010.pdf](http://www.gracelinks.org/media/pdf/freeing_the_grid_2010.pdf).
86. U. S. Environmental Protection Agency Carbon Dioxide Emissions from the Generation of Electric Power in the United States, U.S. DOE, Washington D. C., 2000.
87. S. Farhad, Y. Yoo and F. Hamdullahpur, *J. Power Sources*, 2010, **195**, 1446.
88. C. M. Colson and M. H. Nehrir, *IEEE T. Energy Conver*, 2011, **26**.
89. F. Calise, *Int. J. Hydrogen Energy*, 2011, **36**, 6128.
90. UTC Power: A United Technologies Company, <http://www.utcpower.com/products/purecell400>.
91. B. Godfrey, K. Föger, R. Gillespie, R. Bolden and S. P. S. Badwal, *J. Power Sources*, 2000, **86**, 68.
92. J. Love, R. Ratnaraj, Proceedings of the 6th European Solid Oxide Fuel Cell Forum, Lucerne, Switzerland, 2004.
93. *Gennex brochure*, [http://www.cfcl.com.au/Assets/Files/Gennex\\_Brochure\\_\(EN\)\\_Apr-2010.pdf](http://www.cfcl.com.au/Assets/Files/Gennex_Brochure_(EN)_Apr-2010.pdf), Accessed Jan., 2013.
94. *BlueGen Brochure*, [http://www.bluegen.info/Assets/Files/BlueGen%20Brochure\\_Architects-web.pdf](http://www.bluegen.info/Assets/Files/BlueGen%20Brochure_Architects-web.pdf), Accessed Jan., 2013. .
95. Vaillant Group Presents First Wall-Hung Fuel Cells Heating Appliance, [http://www.vaillant.de/Presse/Press-Releases/article/Vaillant\\_Group\\_presents\\_first\\_wall-hung\\_fuel\\_cells\\_heating\\_appliance](http://www.vaillant.de/Presse/Press-Releases/article/Vaillant_Group_presents_first_wall-hung_fuel_cells_heating_appliance), Accessed Jan. , 2013.

96. *RP1000 & RP1500 Datasheet (1,000 W & 1,500 W Outputs)*, <http://www.acumentrics.com/Collateral/Documents>, Accessed Jan., 2013.
97. *Bloom Energy, ES-5400/ ES-5700 Product Data Sheet*, <http://www.bloomenergy.com/fuel-cell>, Accessed Jan., 2013.
98. DDI Energy, *ARCseriesSOFCInformation3to40kw20120316.pdf*, Accessed Jan., 2013.
99. V. Nerlich, A. Schuler, A. Mai, T. Doerk, Paper presented at: 18th World Hydrogen Energy Conference, Essen, Germany, 2010.
100. Galileo – Decentralised Energy and Heat Supply with Fuel Cells, [www.hexis.com/downloads/hexis\\_prospekt\\_englisch\\_web0703.pdf](http://www.hexis.com/downloads/hexis_prospekt_englisch_web0703.pdf), Accessed Jan., 2013.
101. Information about Fuel Cell Unit Presented at Hannover Messe, <http://fc-district.eu/documents.html> Accessed Jan., 2013.
102. *FC-District*, Presentation on Development of an SOFC Based  $\mu$ -CHP System on Fuel Cell Day, <http://fc-district.eu/documents.html>, Accessed Jan., 2013.
103. O. Bucheli, M. Bertoldi, S. Modena and A. Ravagni, Paper presented at Fuel Cell Seminar, Uncasville, CT, 2012.
104. *Tokyo Gas Webpage-Challenge for the Future Society*, [http://www.tokyo-gas.co.jp/techno/challenge/001\\_e.html](http://www.tokyo-gas.co.jp/techno/challenge/001_e.html), Accessed Jan., 2013.
105. T. Ishikawa, Paper presented at 23rd World Gas Conference, Amsterdam, Netherlands, 2006, <http://www.igu.org/html/wgc2006/pdf/paper/add10759.pdf>.
106. Japanese Group Unveils SOFC Ene-Farm Residential Cogen Unit, *Fuel Cells Bulletin*, 2012, **4**, 4.
107. M. Halinen, J. Saarinen, M. Noponen, I. C. Vinke and J. Kiviaho, *Fuel Cells*, 2010, **10**, 440.
108. M. Halinen, Paper presented at Fuel Cell Seminar, San Antonio, TX, USA, 2010.
109. H. Weineisen, J. Noe, Paper presented at Fuel Cell Seminar, Uncasville, CT, 2012.
110. N. Christiansen, H. Holm-Larsen, S. Primdahl, M. Wandel, S. Ramousse, A. Hagen, *ECS Trans.*, 2011, **35**, 71.
111. M. Powell, K. Meinhardt, V. Sprenkle, L. Chick and G. McVay, *J. Power Sources*, 2012, **205**, 377.
112. D. Engle, *The Journal of Energy Efficiency & Reliability*, 2012, Sep/Oct, **44**.
113. Q. Gu, H. Ren, W. Gao and J. Ren, *Energy and Buildings*, 2012, **51**, 143.
114. U.S. Energy Information Administration, *Quarterly Coal Report January – March 2012*, Washington, D.C., U.S.A., DOE/EIA-0121(2012/01Q), 2012.
115. G. Hale and B. Hobijn, R. Raina, *FRBSF Economic Letter*, 2012, **14**.
116. K. Palmer, D. Burtraw, M. Woerman, B. Beasley. The Effect of Natural Gas Supply on Retail Electricity Prices, Resources for the Future (RFF), Washington D.C., 2012.
117. W. Krewitt, J. Nitsch, M. Fishedick, M. Pehnt and H. Temming, *Energy Policy*, 2006, **34**, 793.

118. E. D. Wachsman, C. A. Marlowe and K. T. Lee, *Energy Environ. Sci.*, 2012, **5**, 5498.
119. J. Warren, S. Das, W. Zhang, Proceedings of the ASME 2012, 10th Fuel Cell Science, Engineering and Technology Conference, San Diego, CA, 2012.
120. S. B. Lee, T. H. Lim, R. H. Song, D. R. Shin and S. K. Dong., *Int. J. Hydrogen Energy*, 2008, **33**, 2330.
121. R. J. Braun, M. Gummalla and J. Yamanis, *J. Fuel Cell Sci. Technol.*, 2009, **6**, 031015–1.
122. P. Nehter, J. B. Hansen and P. K. Larsen, *J. Power Sources*, 2011, **196**, 7347.
123. J. Xu, J. Sui, B. Li and M. Yang, *Energy*, 2010, **35**, 4361.
124. TIAX LLC, Scale-up Study of 5-kW SECA Modules to a 250 kW System, Final report prepared for the U.S. DOE, National Energy Technology Laboratory, 2002.
125. Environmental Protection Agency, Combined Heat and Power: A Clean Energy Solution, U.S.DOE Washington D.C., 2012.
126. National Fuel Cell Research Center, *Build-up of Distributed Fuel Cell Value in California: 2011 Update Background and Methodology*, University of California, Irvine, California, 2011.
127. P. Pehnt, *Int. J. Life. Cycle. Assess.*, 2003, **8**, 283.
128. P. Pehnt, *Int. J. Life. Cycle. Assess.*, 2003, **8**, 365.
129. I. Staffell, A. Ingram and K. Kendall, *Int. J. Hydrogen Energy*, 2012, **37**, 2509.
130. L. S. Schell, *Economic Analysis of Large Stationary Fuel Cell Value in California*, Paper presented at International Colloquium Environmentally Preferred Advanced Power Generation (ICEPAG), Newport Beach, California, CA, 2009.
131. L.S. Schell, *The Cost Effectiveness of DG with and without CHP/CCHP*, Paper presented at International Colloquium Environmentally Preferred Advanced Power Generation (ICEPAG), Costa Mesa, California, CA, 2010.
132. P. R. Epstein, J. J. Buonocore, K. Eckerle, M. Hendryx, B. M. Stout III, R. Heinberg, R. W. Clapp, B. May, N. L. Reinhart, M. M. Ahern, S. K. Doshi and L. Glustrom, *Ann. N. Y. Acad. Sci.*, 2011, **1219**, 73.